

Metadata of the article that will be visualized in OnlineFirst

Please note: Images will appear in color online but will be printed in black and white.

1	Article Title	Pituitary Adenylate Cyclase-Activating Polypeptide (PACAP) Signalling Enhances Osteogenesis in UMR-106 Cell Line
2	Article Sub- Title	
3	Article Copyright - Year	Springer Science+Business Media New York 2014 (This will be the copyright line in the final PDF)
4	Journal Name	Journal of Molecular Neuroscience
5		Family Name Zákány
6		Particle
7		Given Name Róza
8		Suffix
9	Corresponding Author	Organization University of Debrecen
10		Division Department of Anatomy, Histology and Embryology, Faculty of Medicine
11		Address Nagyerdei krt. 98, Debrecen H-4032, Hungary
12		e-mail roza@anat.med.unideb.hu
13		Family Name Juhász
14		Particle
15		Given Name Tamás
16		Suffix
17	Author	Organization University of Debrecen
18		Division Department of Anatomy, Histology and Embryology, Faculty of Medicine
19		Address Nagyerdei krt. 98, Debrecen H-4032, Hungary
20		e-mail
21		Family Name Matta
22		Particle
23		Given Name Csaba
24		Suffix
25	Author	Organization University of Debrecen
26		Division Department of Anatomy, Histology and Embryology, Faculty of Medicine
27		Address Nagyerdei krt. 98, Debrecen H-4032, Hungary
28		e-mail

29 Family Name **Katona**
30 Particle
31 Given Name **Éva**
32 Suffix
33 Author Organization University of Debrecen
34 Division Department of Anatomy, Histology and
Embryology, Faculty of Medicine
35 Address Nagyerdei krt. 98, Debrecen H-4032, Hungary
36 e-mail

37 Family Name **Somogyi**
38 Particle
39 Given Name **Csilla**
40 Suffix
41 Author Organization University of Debrecen
42 Division Department of Anatomy, Histology and
Embryology, Faculty of Medicine
43 Address Nagyerdei krt. 98, Debrecen H-4032, Hungary
44 e-mail

45 Family Name **Takács**
46 Particle
47 Given Name **Roland**
48 Suffix
49 Author Organization University of Debrecen
50 Division Department of Anatomy, Histology and
Embryology, Faculty of Medicine
51 Address Nagyerdei krt. 98, Debrecen H-4032, Hungary
52 e-mail

53 Family Name **Hajdú**
54 Particle
55 Given Name **Tibor**
56 Suffix
57 Author Organization University of Debrecen
58 Division Department of Anatomy, Histology and
Embryology, Faculty of Medicine
59 Address Nagyerdei krt. 98, Debrecen H-4032, Hungary
60 e-mail

61 Author Family Name **Helgadottir**
62 Particle

63		Given Name	Solveig Lind
64		Suffix	
65		Organization	University of Debrecen
66		Division	Department of Anatomy, Histology and Embryology, Faculty of Medicine
67		Address	Nagyerdei krt. 98, Debrecen H-4032, Hungary
68		e-mail	
<hr/>			
69		Family Name	Fodor
70		Particle	
71		Given Name	János
72		Suffix	
73	Author	Organization	University of Debrecen
74		Division	Department of Physiology, Faculty of Medicine
75		Address	Nagyerdei krt. 98, Debrecen H-4032, Hungary
76		e-mail	
<hr/>			
77		Family Name	Csernoch
78		Particle	
79		Given Name	László
80		Suffix	
81	Author	Organization	University of Debrecen
82		Division	Department of Physiology, Faculty of Medicine
83		Address	Nagyerdei krt. 98, Debrecen H-4032, Hungary
84		e-mail	
<hr/>			
85		Family Name	Tóth
86		Particle	
87		Given Name	Gábor
88		Suffix	
89	Author	Organization	University of Szeged
90		Division	Department of Medical Chemistry, Faculty of Medicine
91		Address	Dóm tér 8, Szeged H-6720, Hungary
92		e-mail	
<hr/>			
93		Family Name	Bakó
94		Particle	
95	Author	Given Name	Éva
96		Suffix	
97		Organization	University of Debrecen

98	Division	Cell Biology and Signalling Research Group of the Hungarian Academy of Sciences, Department of Medical Chemistry, Research Centre for Molecular Medicine, Faculty of Medicine
99	Address	Nagyerdei krt. 98, Debrecen H-4032, Hungary
100	e-mail	
101	Family Name	Reglódi
102	Particle	
103	Given Name	Dóra
104	Suffix	
105	Author	Organization
		University of Pécs, Medical School
106	Division	Department of Anatomy, PTE-MTA "Lendület" PACAP Research Team
107	Address	Szigeti út 12, Pécs H-7624, Hungary
108	e-mail	
109	Family Name	Tamás
110	Particle	
111	Given Name	Andrea
112	Suffix	
113	Author	Organization
		University of Pécs, Medical School
114	Division	Department of Anatomy, PTE-MTA "Lendület" PACAP Research Team
115	Address	Szigeti út 12, Pécs H-7624, Hungary
116	e-mail	
117	Received	28 March 2014
118	Schedule	Revised
119	Accepted	22 July 2014
120	Abstract	<p>Presence of the pituitary adenylate cyclase-activating polypeptide (PACAP) signalling has been proved in various peripheral tissues. PACAP can activate protein kinase A (PKA) signalling via binding to pituitary adenylate cyclase-activating polypeptide type I receptor (PAC1), vasoactive intestinal polypeptide receptor (VPAC) 1 or VPAC2 receptors. Since little is known about the role of this regulatory mechanism in bone formation, we aimed to investigate the effect of PACAP on osteogenesis of UMR-106 cells. PACAP 1-38 as an agonist and PACAP 6-38 as an antagonist of PAC1 were added to the culture medium. Surprisingly, both substances enhanced protein expressions of collagen type I, osterix and alkaline phosphatase, along with higher cell proliferation rate and an augmented mineralisation. Although expression of PKA was elevated, no alterations were detected in the expression, phosphorylation and nuclear presence of CREB, but increased</p>

nuclear appearance of Runx2, the key transcription factor of osteoblast differentiation, was shown. Both PACAPs increased the expressions of bone morphogenetic proteins (BMPs) 2, 4, 6, 7 and Smad1 proteins, as well as that of sonic hedgehog, PATCH1 and Gli1. Data of our experiments indicate that activation of PACAP pathway enhances bone formation of UMR-106 cells and PKA, BMP and Hedgehog signalling pathways became activated. We also found that PACAP 6-38 did not act as an antagonist of PACAP signalling in UMR-106 cells.

121	Keywords separated by ' - '	PKA - CREB - Sonic hedgehog - PACAP 6-38 - Mineralisation - Cellular proliferation
122	Foot note information	

Pituitary Adenylate Cyclase-Activating Polypeptide (PACAP) Signalling Enhances Osteogenesis in UMR-106 Cell Line

Tamás Juhász · Csaba Matta · Éva Katona · Csilla Somogyi · Roland Takács ·

Tibor Hajdú · Solveig Lind Helgadottir · János Fodor · László Csernoch ·

Gábor Tóth · Éva Bakó · Dóra Reglódi · Andrea Tamás · Róza Zákány

Received: 28 March 2014 / Accepted: 22 July 2014

© Springer Science+Business Media New York 2014

Abstract Presence of the pituitary adenylate cyclase-activating polypeptide (PACAP) signalling has been proved in various peripheral tissues. PACAP can activate protein kinase A (PKA) signalling via binding to pituitary adenylate cyclase-activating polypeptide type I receptor (PAC1), vasoactive intestinal polypeptide receptor (VPAC) 1 or VPAC2 receptors. Since little is known about the role of this regulatory mechanism in bone formation, we aimed to investigate the effect of PACAP on osteogenesis of UMR-106 cells. PACAP 1-38 as an agonist and PACAP 6-38 as an antagonist of PAC1 were added to the culture medium. Surprisingly, both substances enhanced protein expressions of collagen type I, osterix and alkaline phosphatase, along with higher cell proliferation rate and an augmented mineralisation. Although

expression of PKA was elevated, no alterations were detected in the expression, phosphorylation and nuclear presence of CREB, but increased nuclear appearance of Runx2, the key transcription factor of osteoblast differentiation, was shown. Both PACAPs increased the expressions of bone morphogenetic proteins (BMPs) 2, 4, 6, 7 and Smad1 proteins, as well as that of sonic hedgehog, PATCH1 and Gli1. Data of our experiments indicate that activation of PACAP pathway enhances bone formation of UMR-106 cells and PKA, BMP and Hedgehog signalling pathways became activated. We also found that PACAP 6-38 did not act as an antagonist of PACAP signalling in UMR-106 cells.

28

29

30

31

32

33

34

35

36

37

38

39

Keywords PKA · CREB · Sonic hedgehog · PACAP 6-38 · Mineralisation · Cellular proliferation

40

41

T. Juhász · C. Matta · É. Katona · C. Somogyi · R. Takács ·
T. Hajdú · S. L. Helgadottir · R. Zákány (✉)
Department of Anatomy, Histology and Embryology,
Faculty of Medicine, University of Debrecen,
Nagyterdei krt. 98, H-4032 Debrecen, Hungary
e-mail: roza@anat.med.unideb.hu

J. Fodor · L. Csernoch
Department of Physiology, Faculty of Medicine, University
of Debrecen, Nagyterdei krt. 98, H-4032 Debrecen, Hungary

G. Tóth
Department of Medical Chemistry, Faculty of Medicine,
University of Szeged, Dóm tér 8, H-6720 Szeged, Hungary

É. Bakó
Cell Biology and Signalling Research Group of the Hungarian
Academy of Sciences, Department of Medical Chemistry, Research
Centre for Molecular Medicine, Faculty of Medicine, University of
Debrecen, Nagyterdei krt. 98, H-4032 Debrecen, Hungary

D. Reglódi · A. Tamás
Department of Anatomy, PTE-MTA "Lendület" PACAP Research
Team, University of Pécs, Medical School, Szigeti út 12,
H-7624 Pécs, Hungary

Abbreviations

ALP	Alkaline phosphatase	44
BMP	Bone morphogenetic protein	46
cAMP	Cyclic adenosine monophosphate	48
CNS	Central nervous system	50
CREB	cAMP response element-binding protein	53
DMEM	Dulbecco's modified Eagle's medium	54
dNTP	Deoxynucleotide triphosphate	56
ECM	Extracellular matrix	58
EDTA	Ethylenediaminetetraacetic acid	60
FBS	Foetal bovine serum	63
FGF	Fibroblast growth factor	64
HH	Hedgehog	66
HEPES	4-(2-Hydroxyethyl)- 1-piperazineethanesulfonic acid	68 70
hMSC	Human mesenchymal stem cell	72
IHH	Indian hedgehog	73
MAPK	Mitogen-activated protein kinase	75
MTT	3-(4,5-Dimethylthiazol-2-yl)-2, 5-diphenyltetrazolium bromide	78 79

80	PAC1	Pituitary adenylate cyclase-activating
82		polypeptide type I receptor
83	PACAP	Pituitary adenylate cyclase-activating
85		polypeptide
86	PBS	Phosphate-buffered saline
88	PBST	Phosphate-buffered saline supplemented
90		with 1 % Tween 20
92	PLC	Phospholipase C
93	PKA	Protein kinase A
96	PKC	Protein kinase C
98	PTHrP	Parathyroid hormone-related peptide
900	RT-PCR	Reverse transcription followed
101		by polymerase chain reaction
103	Runx2	Runt-related transcription factor 2
104	SHH	Sonic hedgehog
106	TBE	Tris-boric acid-EDTA
109	TGF β	Transforming growth factor- β
110	VEGF	Vascular endothelial growth factor
113	VIP	Vasoactive intestinal polypeptide
116	VPAC	Vasoactive intestinal polypeptide receptor

117 Introduction

118 Bone formation and regeneration are well-organised processes
 119 orchestrated by several signalling pathways. Initially,
 120 osteoprogenitor cells undergo a rapid proliferation and then
 121 differentiate to early osteoblasts secreting organic bone ma-
 122 trix. In consecutive steps, activity of late osteoblasts results in
 123 an intensive extracellular matrix (ECM) mineralisation and
 124 ultimately osteocytes are formed. Differentiation processes of
 125 osteogenic cells are induced by a few fundamental regulatory
 126 pathways; activation of bone morphogenetic protein (BMP)
 127 (Chen et al. 2012), WNT (Kim et al. 2013), fibroblast growth
 128 factor (FGF) (Marie 2012) and Hedgehog (HH) (Pan et al.
 129 2013) regulated signalling cascades lead to proper bone for-
 130 mation. BMPs, related to the transforming growth factor- β
 131 superfamily (TGF- β), are generally considered as cytokines
 132 regulating various events during embryonic development in-
 133 cluding physiological osteogenesis but also play role in ec-
 134 topic bone formation (Bae et al. 2013). Via the initiation of the
 135 activation of several genes, BMPs are key regulators of ECM
 136 production during bone and cartilage formation both in vitro
 137 and in vivo (Chen et al. 2012; Perrier-Groult et al. 2013;
 138 Zouani et al. 2013). The activation of BMP receptors through
 139 Smads may induce elevated expression of alkaline phosphatase
 140 (ALP) or collagen type I; moreover, it can activate the
 141 expression of bone-specific transcription factors such as
 142 osterix (Wang et al. 2013). Some of these cytokines, including
 143 BMPs 2, 4, 5, 6 and 7 have been identified as markers of
 144 proper osteogenic differentiation, although experimental evi-
 145 dence suggested that a combined expression of these
 146 morphogenes was more essential than the single presence of

any of them (Lavery et al. 2008). One mechanism which may
 result in transcriptional activation of BMP encoding genes is
 the increased activity of protein kinase A (PKA). This kinase
 can phosphorylate cAMP response element-binding protein
 (CREB) transcription factor which subsequently translocates
 into the nucleus and can induce messenger RNA (mRNA)
 expression of BMPs (Zhang et al. 2011). The complexity of
 this regulatory system is hallmarked by the fact that activation
 of genes encoding BMPs can also be regulated by HH signal-
 ling pathway, e.g. via a negative feedback loop of sonic
 hedgehog (SHH) signalling (Bastida et al. 2009; Jiang et al.
 2013). The members of HH family are fundamental regulators
 of various embryonic developmental processes, e.g. neuronal
 differentiation, tooth and limb development (Ehlen et al. 2006;
 Hu et al. 2013; Vazin et al. 2014). The well-balanced spatio-
 temporal expression of HH molecules is crucial during endo-
 chondral ossification both for survival of chondrocytes and for
 induction of their physiological apoptotic program (St-
 Jacques et al. 1999). The elevated expression of Indian hedge-
 hog (IHH) can regulate the expression of parathyroid
 hormone-related peptide (PTHrP) which in turn may upregu-
 late the activation of Runx2 transcription factor, a key player
 of bone formation (Ochiai et al. 2010; St-Jacques et al. 1999).

Pituitary adenylate cyclase-activating polypeptide
 (PACAP), a member of the VIP-secretin-GHRH-glucagon
 superfamily, was originally isolated from extract of rat hypo-
 thalamus (Miyata et al. 1989). The expression of the neuro-
 peptide has been demonstrated in various peripheral organs,
 such as gonads (Reglodi et al. 2012), intestinal tract (Pirone
 et al. 2011) and urinary systems (Gonkowski and Całka 2012),
 and the presence of PACAP has also been verified in human
 milk and blood plasma (Borzsei et al. 2009). The
 posttranslationally modified active form of the neuropeptide
 consists of 38 amino acids, and a shorter 27 amino acid-long
 biologically active variant also exists (Miyata et al. 1989).
 Several in vitro and in vivo data demonstrated the importance
 of PACAP during neuronal differentiation and its general role
 in embryonic development (Ago et al. 2011; Falluel-Morel
 et al. 2008; Ohta et al. 2006). Trophic effect of PACAP has
 been demonstrated in oxidative stress, under ischaemic, toxic
 or traumatic conditions (Horvath et al. 2011; Sanchez et al.
 2008; Shioda et al. 2006; Tamas et al. 2012; Wada et al. 2013).
 The neuropeptide is generally expressed by neurons or re-
 leased in autonomic nerve endings (Braas et al. 1998; Inglott
 et al. 2012), but several nonneuronal cell types such as devel-
 oping germ cells of testis (Shioda et al. 1994), intestinal tissue
 (Pirone et al. 2011) and endothelial cells (Seeliger et al. 2010)
 have also been found to release PACAP. It can bind to three
 specific receptors (pituitary adenylate cyclase-activating poly-
 peptide type I receptor (PAC1), vasoactive intestinal polypep-
 tide receptor (VPAC) 1 and VPAC2 (Jolivel et al. 2009)), from
 which the last two can be activated by both PACAP and VIP
 with equal efficiency, while PAC1 receptor has 100-fold

200	greater affinity to PACAP than VIP (Gourlet et al. 1997).	Administration of PACAP Polypeptides	249
201	Besides these well-characterised members of PACAP signalling pathway, recent data indicated the existence of a novel	PACAP 1-38 at 100 nM (stock solution 100 µM, dissolved in sterile distilled water) was used as agonist of PAC1 receptor;	250
202	PACAP receptor or a novel PACAP receptor-mediated pathway (Jansen-Olesen et al. 2014). The canonical PACAP signalling pathway operates via activation of PAC1 receptor	as an antagonist, PACAP 6-38 at 10 µM (stock solution 10 mM, dissolved in sterile distilled water) was applied continuously from day 1. PACAPs were synthesised as previously described (Jozsa et al. 2005).	251
203	leading to the elevation of intracellular cAMP concentration and consequent activation of PKA signalling (Vaudry et al. 2009). The truncated form of the neuropeptide, PACAP 6-38, having the first five amino acids cleaved down, is regarded as an antagonist of PAC1 receptor (Vandermeers et al. 1992), although its antagonistic effect seems to be tissue and cell type dependent (Reglodi et al. 2008).	Staining Procedures for Light Microscopical Analysis	252
204	Presence of the members of PACAP signalling system has already been demonstrated in different osteogenic cells such as MC3T3 (Nagata et al. 2009) and UMR-106 cells (Kovacs et al. 1996). It has also been shown that PACAP binding can elevate cAMP concentration of UMR-106 cells (Kovacs et al. 1996), and sporadic data prove the importance of the neuropeptide in osteogenesis or bone fracture healing. UMR-106 cell line was originally isolated from rat osteosarcoma. Cells of this cell line can differentiate into osteoblasts after serum withdrawal and show the signs of regular bone formation along with the expression of osteogenic markers and secretion of both organic and inorganic components of bone ECM (Midura et al. 1990; Forrest et al. 1985).	UMR cells of different experimental groups were cultured on round coverslips (Menzel-Gläser, Menzel GmbH, Braunschweig, Germany) placed into Petri dishes (PAA Laboratories). On day 4 or 8, cells were fixed in a 4:1 mixture of absolute ethanol and 40 % formaldehyde. For morphological analysis, cells were stained with haematoxylin-eosin (HE, Sigma-Aldrich, St. Louis, MO, USA); for visualisation of collagen accumulation, Picrosirius red (Sigma-Aldrich) was used; calcium-rich deposits were evaluated with Alizarin red (Sigma-Aldrich); and von Kossa method (Millipore, Billerica, MA, USA) was used to demonstrate appearance of calcium phosphate in cell cultures. All staining protocols were carried out according to the instructions of manufacturer. Photomicrographs were taken using an Olympus DP72 camera on a Nikon Eclipse E800 microscope (Nikon Corporation, Tokyo, Japan).	253
205	In this report, we demonstrate that addition of PACAP neuropeptides enhances bone formation along with elevated nuclear presence of Runx2. PACAPs activate expression of various BMPs and increase the nuclear signal of their downstream target Smad1. Moreover, elevated expression of the components of HH signalling pathways and an enhanced nuclear presence of Gli1 transcription factor is also detected. These observations suggest a multifactorial and dominantly noncanonical PACAP signalling in UMR-106 osteoblastic cells.	Monitoring of Cell Proliferation with ³ H-thymidine Incorporation, Mitochondrial Activity with MTT Assay	254
206		DMEM medium containing 1 µCi/mL ³ H-thymidine (diluted from thymidine [6- ³ H] 20–30 Ci/mmol; 0.74–1.11 TBq/mmol), American Radiolabeled Chemicals, Inc., St. Louis, MO, USA) was added to cell cultures for 16 h on day 4 of culturing. Cells were fixed with ice-cold 5 % trichloroacetic solution for 20 min and were harvested into wells of special opaque 96-well microtitre plates (Wallac, PerkinElmer Life and Analytical Sciences, Shelton, CT, USA). Samples were air-dried for 1 week, and radioactivity was counted by Chameleon liquid scintillation counter (Chameleon, Hidex, Turku, Finland).	255
207		For investigation of general viability or mitochondrial activity, 25 µL 3-[4,5-dimethylthiazolyl-2]-2,5-diphenyltetrazolium bromide (MTT) reagent (25 mg MTT/5 mL PBS) was pipetted into each Petri dish on day 4 of culturing. Cells were incubated for 2 h at 37 °C, followed by addition of 500 µL MTT solubilising solution; absorption of samples was measured at 570 nm (Chameleon, Hidex).	256
208		RT-PCR Analysis	257
209		Cells of UMR-106 cell line were dissolved in TRIzol (Applied Biosystems, Foster City, CA, USA), and after the addition of	258
210			259
211			260
212			261
213			262
214			263
215			264
216			265
217			266
218			267
219			268
220			269
221			270
222			271
223			272
224			273
225			274
226			275
227			276
228			277
229			278
230			279
231			280
232			281
233			282
234			283
235			284
236	Materials and Methods		285
237	Cell Culturing		286
238	Rat osteosarcoma osteoblast-like cell line, UMR-106 (ATCC® CRL-1661™), was used to monitor osteogenic differentiation (Forrest et al. 1985). Cells were cultured in high glucose Dulbecco's modified Eagle's medium (DMEM) (PAA Laboratories, Pasching, Austria) supplemented with 10 % foetal bovine serum (FBS) (PAA Laboratories) at 37 °C in the presence of 5 % CO ₂ and 80 % humidity in a CO ₂ incubator. At 70 % confluence, normal medium was changed to DMEM without FBS for inducing osteogenic differentiation. This day was considered as day 0.		287
239			288
240			289
241			290
242			291
243			292
244			293
245			294
246			
247			
248			

t1.1 **Table 1** Nucleotide sequences, amplification sites, GenBank accession numbers, amplicon sizes and PCR reaction conditions for each primer pair are shown

t1.2	Gene	Primer	Nucleotide sequence (5'→3')	GenBank ID	Annealing temperature	Amplicon size (bp)
t1.3	Alkaline phosphatase (Alpl)	Sense	GAA GTC CGT GGG CAT CGT (474–491)	NM_013059	59 °C	347
t1.4		Antisense	CAG TGC GGT TCC AGA CAT AG (801–820)			
t1.5	BMP2 (Bmp2)	Sense	AAG CCA GGT GTC TCC AAG (697–714)	NM_017178.1	53 °C	209
t1.6		Antisense	AAG TCC ACA TAC AAA GGG TG (886–905)			
t1.7	BMP4 (Bmp4)	Sense	TAG TCC CAA GCA TCA CCC (876–893)	NM_012827.2	53 °C	294
t1.8		Antisense	TCG TAC TCG TCC AGA TAC AAC (1,149–1,169)			
t1.9	BMP6 (Bmp6)	Sense	CCC AGA TTC CTG AGG GTG A (936–954)	NM_013107.1	56 °C	248
t1.10		Antisense	CAT GTT GTG CTG CGG TGT (1,166–1,183)			
t1.11	BMP7 (Bmp7)	Sense	AGG GAG TCC GAC CTC TTC T (607–625)	NM_001191856.1	54 °C	297
t1.12		Antisense	GTT CTG GCT GCG TTG TTT (886–903)			
t1.13	BMPR1 (Bmpr1a)	Sense	CCA TTG CTT TGC CAT TAT (240–257)	NM_009758.4	47 °C	487
t1.14		Antisense	TTT ACC AAC CTG CCG AAC (709–726)			
t1.15	Collagen type I (Coll1a1)	Sense	GGG CGA GTG CTG TGC TTT (348–365)	NM_007742.3	60 °C	388
t1.16		Antisense	GGG ACC CAT TGG ACC TGA A (717–735)			
t1.17	CREB (Creb1)	Sense	AGA TTG CCA CAT TAG CCC (95–112)	NM_031017.1	52 °C	441
t1.18		Antisense	GCT GTA TTG CTC CTC CCT (518–535)			
t1.19	GAPDH (Gapdh)	Sense	TGG CAA AGT GGA GAT TGT TG (69–88)	NM_008084.2	59 °C	486
t1.20		Antisense	GTC TTC TGG GTG GCA GTG AT (535–554)			
t1.21	Gli1 (Gli1)	Sense	CCA CCC TAC CTC TGT CTA TTC G (2,201–2,222)	NM_010296.2	49 °C	423
t1.22		Antisense	CAC CCT TGT TCT GGT TTT ACC (2,603–2,623)			
t1.23	IHH (Ihh)	Sense	CCA ACT ACA ATC CCG ACA TCA (248–268)	NM_053384.1	58 °C	477
t1.24		Antisense	GTC TTC ATC CCA GCC TTC C (390–408)			
t1.25	Osterix (Sp7)	Sense	GCC TAC TTA CCC GTC TGA CTT T (525–543)	NM_001037632.1	56 °C	131
t1.26		Antisense	GCC CAC TAT TGC CAA CTG C (634–652)			
t1.27	PACAP (ADCYAP1)	Sense	GAA GAC GAG GCT TAC GAC CA (314–333)	NM_001001291	56 °C	288
t1.28		Antisense	GTC CGA GTG GCG TTT GGT (584–601)			
t1.29	PAC1 (ADCYAP1R1)	Sense	CTA CGC CCT TTA CTA CCC AG (210–229)	NM_016989.2	49 °C	247
t1.30		Antisense	GTA TTT CTT GAC AGC CAT TTG T (435–456)			
t1.31	PKA (Prkaca)	Sense	GCA AAG GCT ACA ACA AGG C (847–865)	NM_008854	53 °C	280
t1.32		Antisense	ATG GCA ATC CAG TCA ATC G (1,109–1,126)			
t1.33	PKCα (Prkca)	Sense	AGG GAT GAA ATG CGA CAC C (652–670)	NM_001105713.1	55 °C	408
t1.34		Antisense	GAG ACG CCG AAG GAA AGG (1,042–1,059)			
t1.35	PTCH1 (Ptch1)	Sense	TGC TAC AAA TCA GGG GAA CTT (565–585)	NM_053566.1	56 °C	310
t1.36		Antisense	CAG GGC AAT CTG GGT CGG (854–874)			
t1.37	PTHrP (Pthlh)	Sense	CAG ACG ACG AGG GCA GAT (290–307)	NM_012636.1	58 °C	145
t1.38		Antisense	GAC CGA GTC CTT CGC TTT (417–434)			
t1.39	Runx2 (Runx2)	Sense	GGA CGA GGC AAG AGT TTC A (598–616)	NM_001278483.1	55 °C	249
t1.40		Antisense	TGG TGC AGA GTT CAG GGA G (828–846)			
t1.41	SHH (Shh)	Sense	TCG TGC TAC GCA GTC ATC G (1,042–1,060)	NM_017221.1	56 °C	156
t1.42		Antisense	CCT CGC TTC CGC TAC AGA (1,180–1,197)			
t1.43	Smad1 (Smad1)	Sense	AGC ACC TAC CCT CAC TCC C (935–953)	NM_013130.2	56 °C	306
t1.44		Antisense	GAA ACC ATC CAC CAA CAC G (1,222–1,240)			
t1.45	VEGF (Vegfa)	Sense	GCT ACT GCC GTC CGA TTG (1,167–1,184)	NM_001025250.3	54 °C	267
t1.46		Antisense	GCT TTG TTC TGT CTT TCT TTG G (1,412–1,433)			
t1.47	VPAC1 (VIPR1)	Sense	GTT CTA TGG CAC GGT CAA (376–393)	NM_001097523	52 °C	216
t1.48		Antisense	AGC AAT GTT CGG GTT CTC (573–590)			
t1.49	VPAC2 (VIPR2)	Sense	TCG GAA CTA CAT CCA TCT (477–497)	NM_001014970	48 °C	177

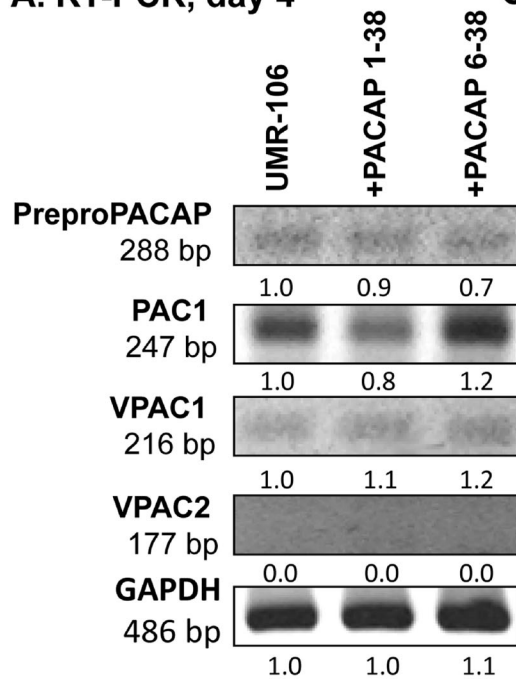
t1.50 **Table 1** (continued)

Gene	Primer	Nucleotide sequence (5'→3')	GenBank ID	Annealing temperature	Amplimer size (bp)
t1.51	Antisense	TTT GCC ATA ACA CCA TAC (636–653)			
295	20 % RNase-free chloroform, samples were centrifuged at		measured by using ImageJ 1.40 g freeware, and results were		316
296	4 °C at 10,000×g for 15 min. Samples were incubated in		normalised to the optical density of untreated control cultures.		317
297	500 µL of RNase-free isopropanol at –20 °C for 1 h; then,				
298	total RNA was harvested in RNase-free water and stored at		Western Blot Analysis		318
299	–20 °C. The assay mixture for reverse transcriptase reaction				
300	contained 2 µg RNA, 0.112 µM oligo(dT), 0.5 mM		Cells were washed in physiological NaCl solution and were		319
301	deoxynucleotide triphosphate (dNTP), 200 units of High		harvested. After centrifugation, cell pellets were suspended in		320
302	Capacity RT (Applied Bio-Systems) in 1× RT buffer. For the		100 µL of homogenisation radio immunoprecipitation assay		321
303	sequences of primer pairs and further details of polymerase		(RIPA) buffer (150 mM sodium chloride; 1.0 % NP ₄₀ , 0.5 %		322
304	chain reactions, see Table 1. Amplifications were performed		sodium deoxycholate; 50 mM Tris, pH 8.0) containing prote-		323
305	in a thermal cycler (Labnet MultiGene™ 96-well Gradient		ase inhibitors (aprotinin (10 µg/mL), 5 mM benzamidine,		324
306	Thermal Cycler; Labnet International, Edison, NJ, USA) in a		leupeptin (10 µg/mL), trypsin inhibitor (10 µg/mL), 1 mM		325
307	final volume of 21 µL (containing 1 µL forward and reverse		PMSF, 5 mM EDTA, 1 mM EGTA, 8 mM Na fluoride, 1 mM		326
308	primers [0.4 µM], 0.5 µL dNTP [200 µM], and 5 units of		Na orthovanadate). Samples were stored at –70 °C.		327
309	Promega GoTaq® DNA polymerase in 1× reaction buffer) as		Suspensions were sonicated by pulsing burst for 30 s at 40		328
310	follows: 95 °C, 2 min, followed by 35 cycles (denaturation,		A (Cole-Parmer, IL, USA). For Western blotting, total cell		329
311	94 °C, 1 min; annealing at optimised temperatures as given in		lysates were used. Samples for sodium dodecyl sulfate poly-		330
312	Table 1 for 1 min; extension, 72 °C, 90 s) and then 72 °C,		acrylamide gel electrophoresis (SDS-PAGE) were prepared		331
313	10 min. PCR products were analysed by electrophoresis in		by the addition of Laemmli electrophoresis sample buffer		332
314	1.2 % agarose gel containing ethidium bromide. GAPDH was		(4 % SDS, 10 % 2-mercaptoethanol, 20 % glycerol, 0.004 %		333
315	used as internal control. Optical density of signals was		bromophenol blue, 0.125 M Tris–HCl pH 6.8) to cell lysates		334

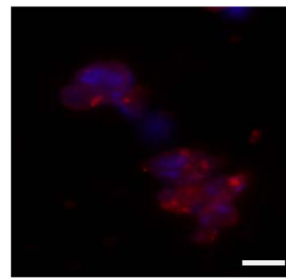
t2.1 **Table 2** Tables of antibodies
t2.2 used in the experiments

	Antibody	Host animal	Dilution	Distributor
t2.3	Anti-PAC1	Rabbit, polyclonal	1:600	Sigma-Aldrich, St. Louis, MO, USA
t2.4	Anti-PKA	Rabbit, polyclonal	1:600	Cell Signaling, Danvers, MA, USA
t2.5	Anti-CREB	Rabbit, polyclonal	1:800	Millipore, Billerica, MA, USA
t2.6	Anti-p-CREB	Rabbit, polyclonal	1:800	Millipore, Billerica, MA, USA
t2.7	Anti-Coll. I.	Mouse, monoclonal	1:1,000	Sigma-Aldrich, St. Louis, MO, USA
t2.8	Anti-osterix	Goat, polyclonal	1:200	Santa Cruz Biotechnology, Dallas, TX, USA
t2.9	Anti-ALP	Rabbit, polyclonal	1:600	Abcam, Cambridge, UK
t2.10	Anti-Runx2	Rabbit, polyclonal	1:600	Cell Signaling, Danvers, MA, USA
t2.11	Anti-PKCα	Rabbit, polyclonal	1:600	Cell Signaling, Danvers, MA, USA
t2.12	Anti-BMP2	Rabbit, polyclonal	1:400	Abcam, Cambridge, UK
t2.13	Anti-BMP4	Rabbit, polyclonal	1:600	Cell Signaling, Danvers, MA, USA
t2.14	Anti-BMP6	Goat, polyclonal	1:200	Santa Cruz Biotechnology, Dallas, TX, USA
t2.15	Anti-BMP7	Rabbit, polyclonal	1:600	Abcam, Cambridge, UK
t2.16	Anti-BMPRI	Mouse, monoclonal	1:600	Abcam, Cambridge, UK
t2.17	Anti-Smad1	Rabbit, polyclonal	1:600	Cell Signaling, Danvers, MA, USA
t2.18	Anti-SHH	Rabbit, polyclonal	1:600	Cell Signaling, Danvers, MA, USA
t2.19	Anti-IHH	Rabbit, polyclonal	1:600	Millipore, Billerica, MA, USA
t2.20	Anti-PTHrP	Mouse, monoclonal	1:300	R&D Systems, Minneapolis, MN, USA
t2.21	Anti-PTCH1	Rabbit, polyclonal	1:600	Abcam, Cambridge, UK
t2.22	Anti-Gli1	Rabbit, polyclonal	1:600	Cell Signaling, Danvers, MA, USA
t2.23	Anti-GAPDH	Rabbit, polyclonal	1:1,000	Abcam, Cambridge, UK

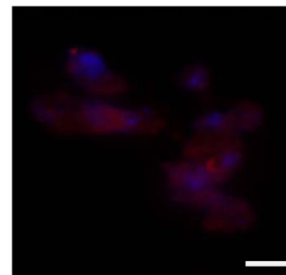
A. RT-PCR, day 4



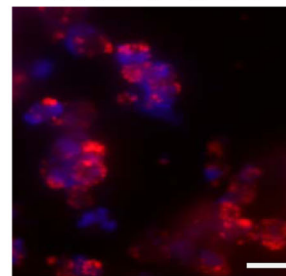
C. Immunocytochemistry, day 4, PAC1



UMR-106

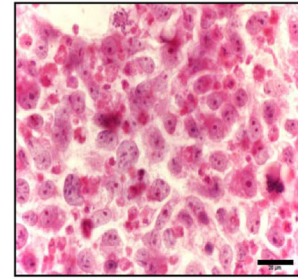


+PACAP 1-38

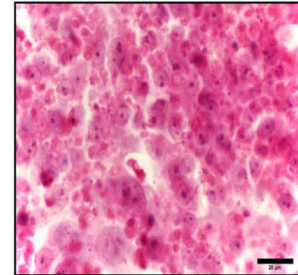


+PACAP 6-38

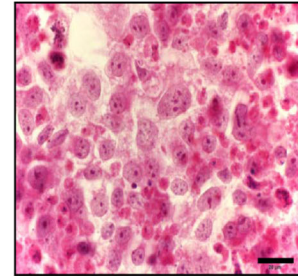
D. Haematoxylin Eosin staining, day 4



UMR-106

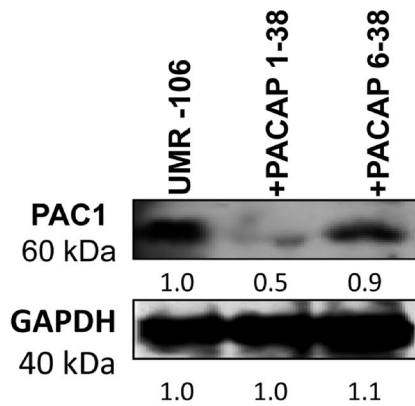


+PACAP 1-38

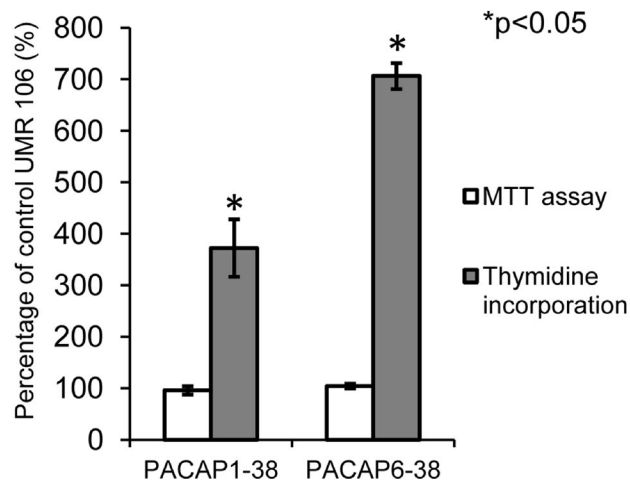


+PACAP 6-38

B. Western blot, day 4



E. Mitochondrial activity and cellular proliferation, day 4



◀ **Fig. 1** Effects of PACAP on receptor expression, morphology, mitochondrial or proliferation activity of UMR-106 cells. mRNA (**a**) and protein (**b**) expression of preproPACAP and PACAP receptors in UMR-106 cell line. For RT-PCR and Western blot reactions, GAPDH was used as controls. Integrated optical densities of signals were determined by ImageJ software, and the results were normalised to the optical density of control cultures. Representative data of three independent experiments are shown. **c** Immunocytochemistry of PAC1 receptor in UMR-106 cells on day 4 of culturing. Original magnification was $\times 60$. *Scale bar* 10 μm . **d** Morphology of 4-day-old UMR-106 cells was visualised with haematoxylin-eosin (HE) staining. Original magnification was $\times 40$. *Scale bar* 20 μm . **e** Effects of PACAP administration on mitochondrial metabolic activity (MTT) and cellular proliferation (^3H -thymidine incorporation) in UMR-106 cell line on culturing day 4. *Asterisks* indicate significant ($*p < 0.05$) alteration of cell proliferation as compared to the respective control

335 to set equal protein concentration of samples, and boiled for
336 10 min. About 40 μg of protein was separated by 7.5 % SDS-
337 PAGE gel for detection of PAC1, PKA, GAPDH, CREB, p-
338 CREB, Coll. I, osterix, ALP, Runx2, PKC α , BMP2, BMP4,
339 BMP6, BMP7, BMPR1, Smad1, PTHrP, SHH, IHH, PTCH1
340 and Gli1. Proteins were transferred electrophoretically to ni-
341 trocellulose membranes. After blocking with 5 % nonfat dry
342 milk in phosphate-buffered saline with 0.1 % Tween 20
343 (PBST), membranes were washed and exposed to the primary
344 antibodies overnight at 4 $^{\circ}\text{C}$ in the dilution as given in Table 2.
345 After washing for 30 min in PBST, membranes were incubat-
346 ed with anti-rabbit IgG (Bio-Rad Laboratories, CA, USA) in
347 1:1,500, anti-goat IgG (Sigma) in 1:2,000 and anti-mouse IgG
348 (Bio-Rad Laboratories) in 1:1,500 dilution. Signals were de-
349 tected by enhanced chemiluminescence (Pierce) according to
350 the instructions of the manufacturer. Signals were manually
351 developed on X-ray films (Agfa-Gevaert Group, Mortsel,
352 Belgium). Optical density of Western blot signals was mea-
353 sured by using ImageJ 1.40 g freeware, and results were
354 normalised to that of untreated control cultures.

355 Immunocytochemistry

356 On day 4, immunocytochemistry was performed on cells cul-
357 tured on the surface of coverslips to visualise the intracellular
358 localisation of PAC1, p-CREB, Runx2, Smad1 and Gli1.
359 Extracellular organisation of collagen type I was also monitored
360 by immunohistochemical staining. Cells were fixed in Saint-
361 Marie's fixative (99 % ethanol and 1 % anhydrous acetic acid)
362 and washed in 70 % ethanol. After rinsing in PBS (pH 7.4),
363 nonspecific binding sites were blocked with PBST supplement-
364 ed with 1 % bovine serum albumin (Amresco LLC, Solon, OH,
365 USA); then, cultures were incubated with polyclonal anti-PAC1
366 antibody (Sigma), polyclonal Runx2 (Cell Signaling), Gli1
367 (Cell Signaling), Smad1 (Cell Signalling) and p-CREB
368 (Millipore) antibodies at a dilution of 1:400 and monoclonal
369 anti-Coll. I. (Sigma) antibody at a dilution of 1:800 at 4 $^{\circ}\text{C}$
370 overnight. Primary antibodies were visualised with anti-rabbit
371 Alexa555 or anti-mouse Alexa555 secondary antibodies (Life

Technologies Corporation, Carlsbad, CA, USA) at a dilution of 372
1:1,000. Specificity of antibodies was confirmed by applying 373
control peptides that were identical to antigens against which the 374
antibodies were raised; in these experiments, no specific signals 375
were detected (data not shown). Cultures were mounted in 376
Vectashield mounting medium (Vector Laboratories, 377
Peterborough, England) containing DAPI for nuclear DNA 378
staining. Photomicrographs of the cultures were taken using 379
an Olympus DP72 camera on a Nikon Eclipse E800 microscope 380
(Nikon Corporation, Tokyo, Japan). Images were acquired 381
using cellSense Entry 1.5 software (Olympus, Shinjuku, 382
Tokyo, Japan) using constant camera settings to allow compar- 383
ison of fluorescent signal intensities. For investigation of sub- 384
cellular localisation of p-CREB, Runx2, Gli1 and PAC1, fluo- 385
rescent images were also taken with an Olympus FV1000S 386
confocal microscope (Olympus Co., Tokyo, Japan) using $\times 60$ 387
oil immersion objective (NA: 1.3). For excitation, laser line of 388
543 nm was used. The average pixel time was 4 μs . Z image 389
series of 1- μm optical thickness were recorded in sequential 390
scan mode. Images of Alexa555 and DAPI were overlaid using 391
Adobe Photoshop version 10.0 software. Optical density of 392
fluorescent signals was measured by using ImageJ 1.40 g free- 393
ware, and the data were compared to that of untreated control 394
cultures. Integrated optical density of nuclei of 30 independent 395
cells in randomly chosen field of view was calculated. 396

PKC Activity Assay 397

398 Cells were washed in physiological NaCl solution and were
399 harvested. After centrifugation, cell pellets were suspended in
400 100 μL of homogenisation RIPA buffer containing protease
401 inhibitors mentioned above. Suspensions were sonicated by
402 pulsing burst for 3×10 s at 40 A (Cole-Parmer) on ice. After
403 centrifugation at $10,000 \times g$ for 10 min at 4 $^{\circ}\text{C}$, supernatants of
404 samples were used for in vitro enzyme activity measurements.
405 Untreated cultures were used as controls. Gö 6976 was added
406 as classical PKC inhibitor, the activity decrease of all PKC
407 isotypes considered as classical PKC activity. Measurements
408 were performed according to Huang and Huang (1991).

Determination of Cytosolic Free Ca^{2+} Concentration 409

410 Measurements were performed on day 2 on cultures seeded
411 onto 30-mm round coverslips using the calcium-dependent
412 fluorescent dye Fura-2 as described previously (Matta et al.
413 2008). Fura-2-loaded cells were placed on the stage of an
414 inverted fluorescent microscope (Diaphot, Nikon, Kowasaki,
415 Japan) and viewed using a $\times 40$ oil immersion objective.
416 Measurements were carried out in Tyrode's salt solution (con-
417 taining 1.8 mM Ca^{2+} ; composition 137 mM NaCl, 5.4 mM
418 KCl, 0.5 mM MgCl_2 , 1.8 mM CaCl_2 , 11.8 mM HEPES, 1 g/L
419 glucose; pH 7.4) in a perfusion chamber using a dual wave-
420 length monochromator equipment (DeltaScan, Photon

Technologies International, Lawrenceville, KY, USA) at room temperature. Excitation wavelength was altered between 340 and 380 nm at 50 Hz, and emission wavelength was detected at 510 nm. Data acquisition frequency was 10 Hz. Ratios of emitted fluorescence intensities (detected at alternating excitation wavelengths; F_{340}/F_{380}) were measured as previously described (Matta et al. 2008). Basal cytosolic Ca^{2+} concentration was determined on day 2 directly after PACAP administration in three independent experiments, measuring 10 cells in each case.

Statistical Analysis

All data are representative of at least three different experiments. Where applicable, data are expressed as mean \pm SEM. Statistical analysis was performed by Student's *t* test where statistical method reported significant differences among the groups at $p < 0.05$.

Results

PACAP Neuropeptides Act on PAC1 Receptor and Increase Proliferation of UMR-106 Cells

Weak signals of preproPACAP mRNA were detected in UMR-106 cells without any significant alteration when PACAP treatments were applied. Out of the three PACAP receptors, obvious mRNA expression of PAC1 and weaker signals of VPAC1 mRNA were found, while expression of VPAC2 mRNA remained undetectable. PACAP treatments did not cause any significant alterations of these signals (Fig. 1a). Expression of PAC1 protein was detected on Western blot and treatment with PACAP 1-38 gave rise to a moderate decrease of its signal, while PACAP 6-38 did not have any significant influence on the PAC1 protein level (Fig. 1b). Presence of PAC1 receptor was also demonstrated with immunocytochemistry and stronger fluorescent signals appeared by the addition of PACAP 6-38 (Fig. 1c).

Morphology and viability of UMR-106 cells were not altered by the addition of PACAP neuropeptides to the cell cultures (Fig. 1d, e), but significantly increased proliferation was observed. Continuous application of PACAP 1-38 at 100 nM for 4 days resulted in an approximately 400 % elevation of proliferation rate and surprisingly PACAP 6-38, accepted as an antagonist of PAC1 receptor, exerted an even stronger stimulatory effect on cell proliferation (Fig. 1e).

Osteogenic Differentiation Was Enhanced After PACAP Addition

In the next step of our experiments, we aimed to investigate the effect of PACAP treatments on bone formation. To this

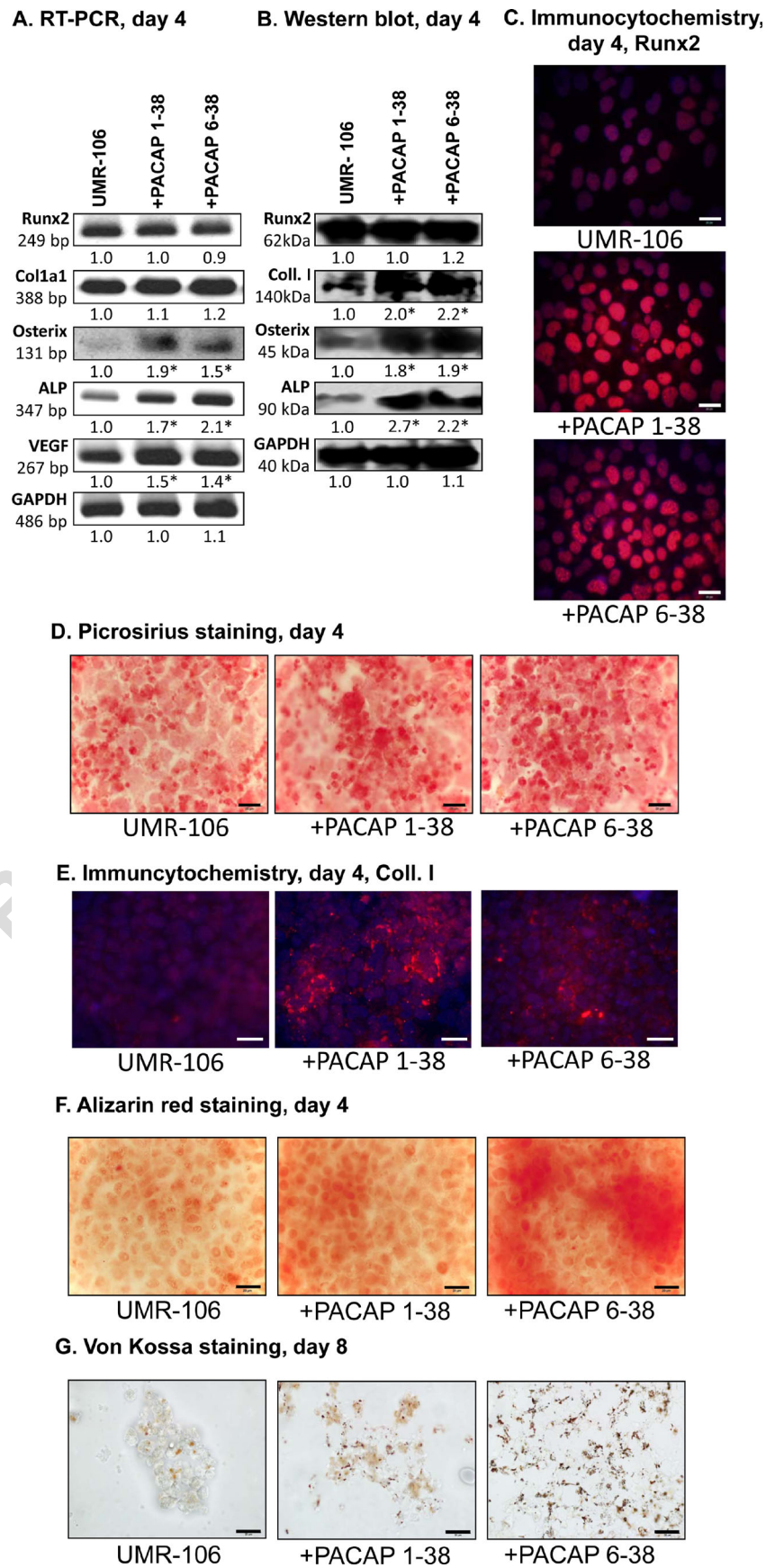
end, we performed RT-PCRs and Western blots of various osteogenesis markers. Administration of PACAPs did not cause any significant change in the mRNA and protein expression profile of Runx2 (Fig. 2a, b), although the nuclear appearance of this osteogenic transcription factor became more pronounced under the effect of PACAP neuropeptides, as it was revealed by immunocytochemistry (Fig. 2c). Nuclear activity of Runx2 may result in an elevation of bone-specific extracellular matrix production. Indeed, an elevated protein level of collagen type I, the major organic component of bone matrix, was detected with Western blots (Fig. 2b). Accumulation of collagen in extracellular space was confirmed with Picosirius red staining (Fig. 2d) and immunocytochemistry of collagen type I (Fig. 2e) as the result of PACAP treatment. Osterix is another key transcription factor during osteogenesis, characteristic for more advanced stages of bone formation. mRNA and protein expression of osterix showed approximately a 2-fold elevation at the presence of PACAPs (Fig. 2a, b). Later stages of bone formation are characterised by beginning of matrix mineralisation, and indeed, elevated mRNA and protein expression of ALP and an increased mRNA expression of VEGF were found (Fig. 2a, b).

Mineralisation of bone matrix begins with accumulation of Ca^{2+} salts and continues with deposition of phosphates in the extracellular space. In order to detect these inorganic bone matrix constituents, we performed Alizarine red staining to demonstrate calcification and von Kossa reactions to investigate deposition of phosphates. Both PACAPs elevated the extracellular calcium deposits in cell cultures' UMR-106 cell line investigated on day 4 of culturing, and this effect was more pronounced in case of the application of PACAP 6-38 (Fig. 2f). No positive signals were detected with von Kossa staining on day 4 of culturing (data are not shown), but both neuropeptides elevated the extracellular phosphate accumulation comparing with the untreated control by day 8 of culturing; effect of PACAP 6-38 was stronger again, compared to that of PACAP 1-38 (Fig. 2g). As a very surprising and unexpected result of these experiments, although PACAP 6-38 is believed as an antagonist of PAC1 receptor, it exerted positive effects on osteogenesis, similar to the application of the PAC1 receptor agonist, PACAP 1-38.

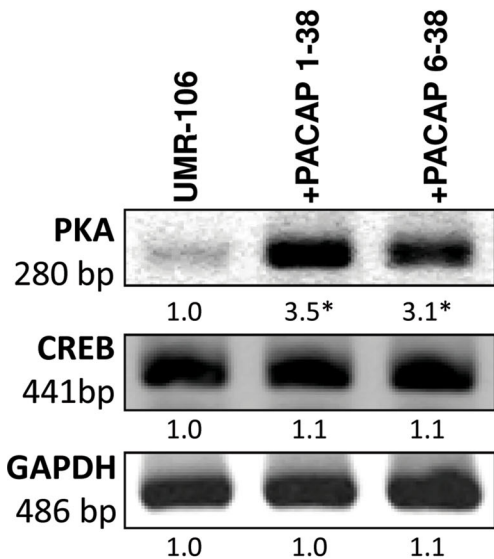
Canonical PKA-Mediated Downstream Signalling Pathway Showed Only Partial Activation Under the Effect of PACAPs

In further steps of our experiments, we aimed to clarify downstream signalling mechanisms evoked by PACAPs and resulting in enhanced bone formation. The canonical downstream pathway of PAC1 receptor activation is the cAMP-dependent PKA signalling via CREB phosphorylation. In line with the previously described osteogenesis-promoting effect, both PACAP neuropeptides were found to induce significant

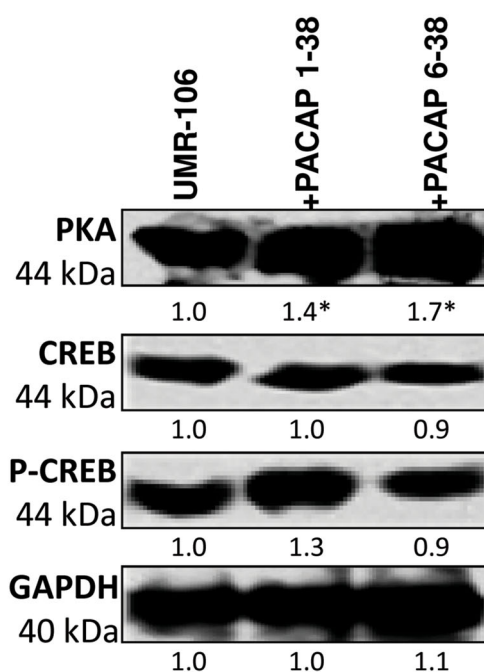
Fig. 2 PACAP influence Runx2, Coll. I, osterix, ALP and VEGF expression in UMR-106 cells. mRNA (a) and protein (b) expression of Runx2, Coll. I, osterix, ALP and VEGF in UMR-106 cells on day 4 of culturing. For RT-PCR and Western blot reactions, GAPDH was used as controls. Optical density of signals was measured, and the results were normalised to the optical density of controls. **a**, **b**, Numbers below signals represent integrated densities of signals determined by ImageJ software. **c** Immunocytochemistry of Runx2 in UMR-106 cells on day 4 of culturing. Original magnification was $\times 60$. Scale bar 20 μm . **d** Collagen in 4-day-old UMR-106 cell culture was visualised with Picosirius staining. Original magnification was $\times 40$. Scale bar 20 μm . **e** Immunocytochemistry of collagen type I in 4-day-old UMR-106 cell cultures. Original magnification was $\times 100$. Scale bar 20 μm . **f** Extracellular Ca^{2+} deposits of 4-day-old UMR-106 cells were visualised with Alizarin red staining. Original magnification was $\times 40$. Scale bar 20 μm . **g** Extracellular Ca^{2+} phosphate crystals were detected with von Kossa method on day 8 of culturing. Original magnification was $\times 40$. Scale bar 20 μm . Asterisks indicate significant ($*p < 0.05$) alteration of expression as compared to the respective control. Representative data of three independent experiments are shown



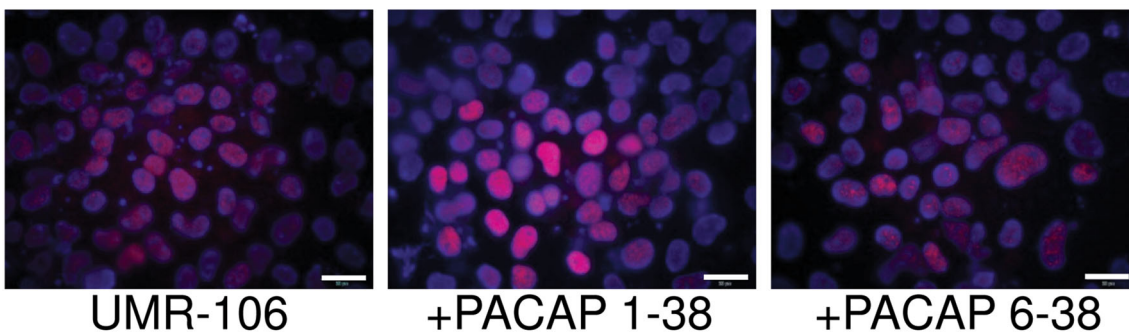
A. RT-PCR, day 4



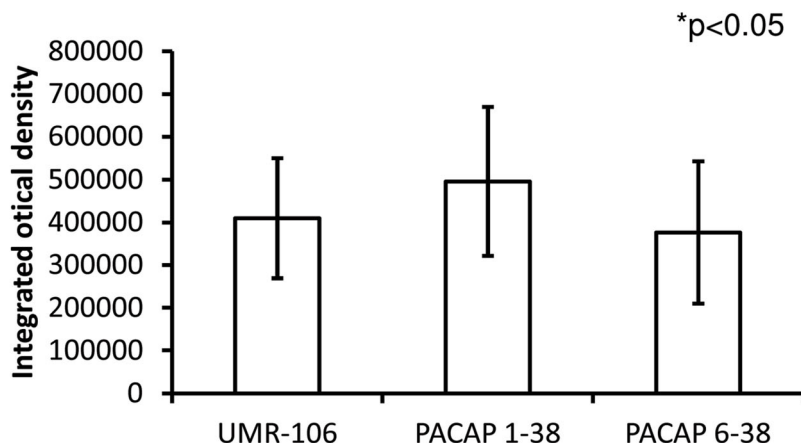
B. Western blot, day 4



C. Immunocytochemistry, day 4, P-CREB



D. Densitometry of P-CREB immunocytochemistry, day 4



518 elevation either mRNA or protein levels of PKA (Fig. 3a, b).
 519 CREB transcription factor is the major downstream effector of

PKA signalling; thus, we investigated the possible changes of
 its expression and phosphorylation. Although elevation of

◀ **Fig. 3** PACAP augments PKA expression without affecting CREB phosphorylation in UMR-106 cells. mRNA (a) and protein (b) expression of PKA, CREB and p-CREB in UMR-106 cells on day 4 of culturing. For RT-PCR and Western blot reactions, GAPDH was used as controls. Optical density of signals was measured, and the results were normalised to the optical density of controls. **a, b** Numbers below signals represent integrated densities of signals determined by ImageJ software. **c** Immunocytochemistry of p-CREB in UMR-106 cells on day 4 of culturing. Original magnification was $\times 60$. Scale bar 20 μm . **d** Integrated density of nuclei of 30 independent cells in randomly selected field of view was measured. Analysis of fluorescent signal of nuclei of PACAP treated and 30 control cells of three independent experiments was performed, respectively. Asterisks indicate significant ($*p < 0.05$) alteration of expression as compared to the respective control. Representative data of three independent experiments are shown

522 expression and/or phosphorylation of CREB could be anticipated, we failed to detect any significant change of these
523 parameters under the effect of PACAPs (Fig. 3a, b). To confirm
524 these unexpected results, we performed immunocytochemistry,
525 and indeed, we did not observe any significant change in the
526 nuclear signal of p-CREB in PACAP-treated cells as it was
527 demonstrated with densitometry of immunofluorescent signals
528 detected at nuclear area of cells (Fig. 3c, d).
529

530 Ca^{2+} -Induced PKC-Mediated PACAP Signalling Pathway 531 Was Not Activated

532 After being unable to prove any significant activation of
533 PACAP-related CREB phosphorylation, we turned our attention
534 to explore whether the Ca^{2+} -dependent effector mechanisms
535 responded to the presence of the neuropeptides. PAC1 receptor
536 may signal towards PLC pathway activation, through which it
537 can regulate IP_3 operated release of Ca^{2+} from internal
538 stores and in turn can activate PKC (Osipenko et al. 2000).
539 Resting intracellular Ca^{2+} concentration of UMR-106 cells
540 was monitored first, and we found that PACAP treatment
541 did not result in any significant change of this parameter
542 (Fig. 4a). No alterations were detected either in the mRNA
543 or protein expression of $\text{PKC}\alpha$ (Fig. 4b, c); furthermore, we
544 also failed to detect any significant change in the activity of
545 classical PKCs following PACAP administration (Fig. 4d).

546 Regulation of BMP Expression is Involved in PACAP 547 Downstream Signalling Pathways

548 As we failed to detect any significant response of CREB and
549 cPKC as a result of PACAP treatments, we tried to identify
550 other osteogenesis-related signalling mechanisms which could
551 be responsible for the elevated expression of ALP and osterix
552 observed after PACAP treatments. As BMPs can stimulate
553 osteoblast differentiation and bone formation, we investigated
554 the responsiveness of the members of this signalling pathway to
555 PACAP treatments. Elevated protein expressions of BMPs 2, 4,
556 6 and 7 were detected along with inconsistent alterations of

mRNA expressions under the effect of PACAP treatments 557
(Fig. 5a, b). BMPs 2, 4, 6 and 7 can exert their biological 558
effects via binding primarily to BMPRI, and this interaction 559
results in activation of members of R-Smad transcription factor 560
family. We found that UMR-106 cells express mRNA and 561
protein of BMPRI, and either expression remained constant 562
under the effect of PACAP treatments (Fig. 5a, b). Smad1 is 563
one of the downstream targets of BMP signalling. Expression 564
either of Smad1 mRNA or protein became significantly elevated 565
(Fig. 5a, b). We also detected enhanced immunofluorescent 566
signals of Smad1 following of PACAP treatments, when nuclear 567
presence of this transcription factor was investigated with 568
immunocytochemistry (Fig. 5c). We also compared the nuclear 569
intensity of Smad1 immunofluorescent signals detected in 570
PACAP-treated cells with that of the untreated control cells, 571
and a significantly elevated nuclear presence of Smad1 trans- 572
cription factor was proved (Fig. 5d). 573

574 HH Signalling Pathways Were Activated During PACAP 575 Administration

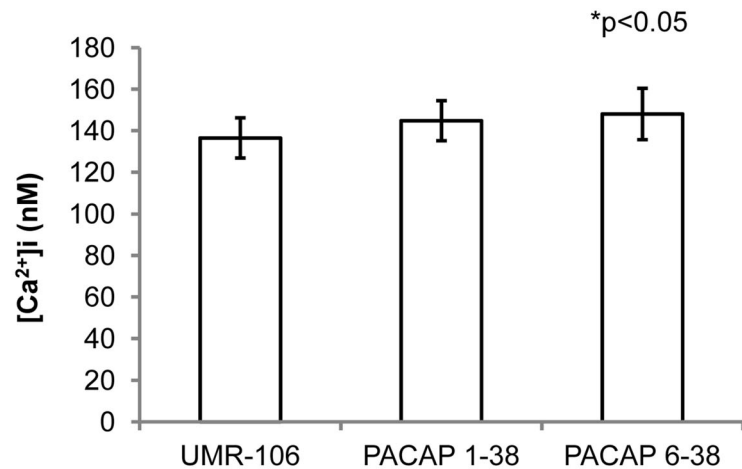
576 Despite having an intimate cross talk between Runx2 and
577 BMP pathways, osteogenesis is also characterised by the
578 connection of these signalling mechanisms with other
579 morphogenes. One of the major candidates of this link is the
580 HH signalling pathway, which can regulate BMP expression
581 and/or proliferation of cells. The balance between the activity
582 of IHH and PTHrP is a key factor of bone formation. In UMR-
583 106 cells, the mRNA and protein expression of IHH remained
584 at a constant level after PACAP administration while both of
585 the mRNA and protein expression of PTHrP elevated significantly
586 (Fig. 6a, b). mRNA and protein expression of SHH
587 was also detected in UMR-106 cells, and either signals
588 showed strong elevation after treatments with PACAPs
589 (Fig. 6a, b). The mRNA expression of PTCH1, the receptor
590 of SHH and/or IHH, was not altered by PACAPs, but its
591 protein expression became elevated by the neuropeptide treat-
592 ments (Fig. 6a, b). Ligand binding of PTCH1 ultimately
593 induces activation of Gli1 transcription factor; therefore, we
594 investigated the presence and subcellular localisation of this
595 signalling molecule. In line with the elevation of SHH protein
596 level, stronger bands for Gli1 protein were detected in Western
597 blots (Fig. 6a, b) and enhanced nuclear signals were observed
598 with immunocytochemistry (Fig. 6c) upon PACAP treat-
599 ments. This elevation proved to be significant with densitom-
600 etry of nuclear Gli1 fluorescent signals (Fig. 6d).

602 Discussion

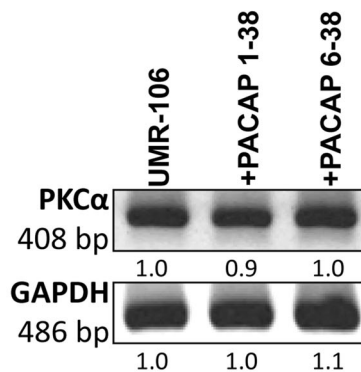
603 PACAP neuropeptide is a well-known regulator of neurogenic
604 differentiation and/or migration; therefore, its presence is es-
605 sential for proper central nervous system formation (Toriyama

Fig. 4 Effects of PACAPs on intracellular Ca^{2+} of UMR-106 cells. **a** Basal cytosolic Ca^{2+} concentration in Fura-2-loaded cells on day 4 of culturing. Measurements were carried out in untreated control cultures and during PACAP treatments. Data shown are mean values of ten cells in each experimental group. **b** mRNA and **c** protein expression of PKC α in UMR-106 cells on day 4 of culturing. GAPDH was used as a control. *Numbers below signals* represent integrated densities of signals determined by ImageJ software. **d** Enzyme activity of classical PKC in UMR-106 cells on day 4. *Asterisks* indicate significant ($*p < 0.05$) increase of expression or activity as compared to the respective control. Representative data of three independent experiments are shown

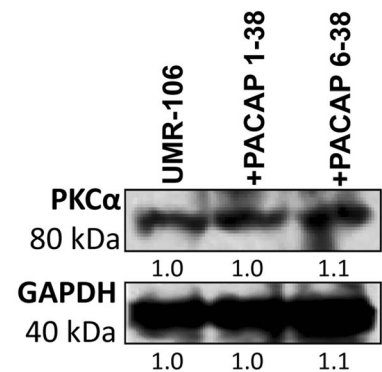
A. Resting ic Ca^{2+} concentration, day 4



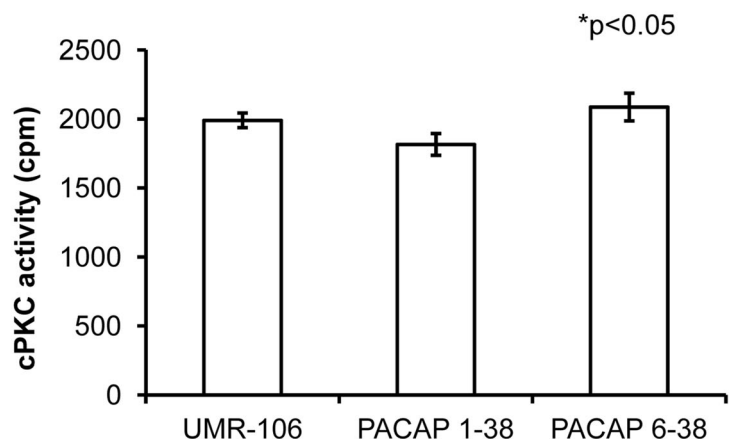
B. RT-PCR, day 4



C. Western blot, day 4



D. cPKC activity, day 4

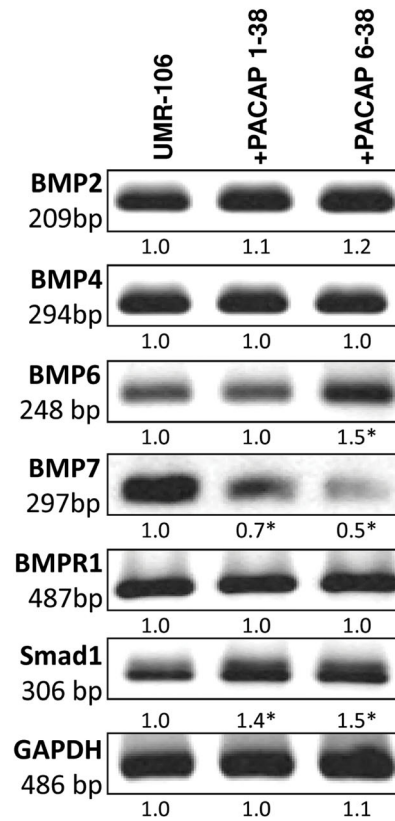


606 et al. 2012; Vaudry et al. 2009; Watanabe et al. 2007). In the
 607 last decade, increasing number of experiments have been
 608 performed proving presence of the neuropeptide in

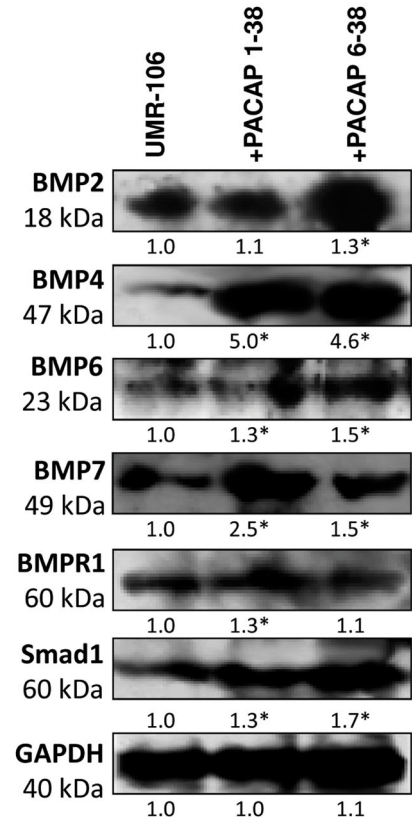
609 nonneuronal organs and tissues, such as intestinal tract
 610 (Pirone et al. 2011), gonads (Shpakov et al. 2011) or even in
 611 blood (Reglodi et al. 2010). Although a substantial amount of

Fig. 5 Administration of PACAPs activates BMP signalling of UMR-106 cells. mRNA (a) and protein (b) expression of BMP2, BMP4, BMP6, BMP7, BMPR1 and Smad1 in UMR-106 cells on day 4 of culturing. For RT-PCR and Western blot reactions, GAPDH was used as control. Optical density of signals was measured, and the results were normalised to the optical density of controls. **a**, **b** Numbers below signals represent integrated densities of signals determined by ImageJ software. **c** Immunocytochemistry of Smad1 in UMR-106 cells on day 4 of culturing. Original magnification was $\times 60$. Scale bar 5 μm . **d** Integrated density of nuclei of 30 independent cells in randomly selected field of view was measured. Analysis of fluorescent signal of nuclei of PACAP treated and 30 control cells of three independent experiments was performed, respectively. Asterisks indicate significant ($*p < 0.05$) alteration of expression as compared to the respective control. Representative results of three independent experiments are shown

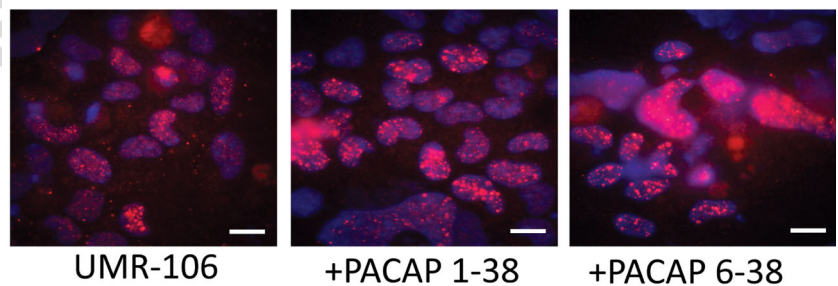
A. RT-PCR, day 4



B. Western blot, day 4



C. Immunocytochemistry, day4, Smad1



D. Densitometry of immunocytochemistry, day4, Smad1

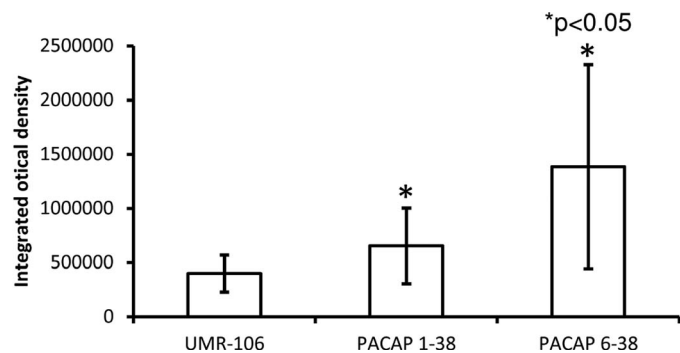
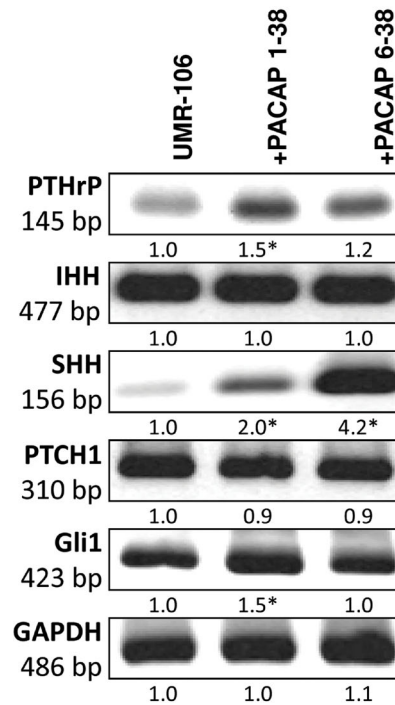
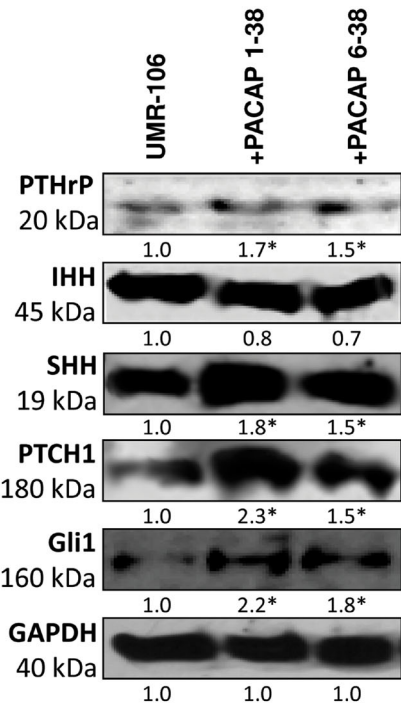


Fig. 6 Effects of PACAPs on HH signalling of UMR-106 cells. PACAP 1-38 at 100 nM and PACAP 6-38 at 10 μ M were administrated continuously from day 1. mRNA (a) and protein (b) expression of IHH, PTHrP, SHH, PTCH1 and Gli1 in UMR-106 cells on day 4 of culturing. For RT-PCR and Western blot reactions, GAPDH was used as controls. Optical density of signals was measured, and the results were normalised to the optical density of controls. **a, b** Numbers below signals represent integrated densities of signals determined by ImageJ software. **c** Immunocytochemistry of Gli1 in UMR-106 cells on day 4 of culturing. Original magnification was $\times 60$. Scale bar 5 μ m. **d** Integrated density of nuclei of 30 independent cells in randomly selected field of view was measured. Analysis of fluorescent signal of nuclei of PACAP treated and 30 control cells of three independent experiments was performed, respectively. Asterisks indicate significant ($*p < 0.05$) alteration of expression as compared to the respective control. Representative data of three independent experiments are shown

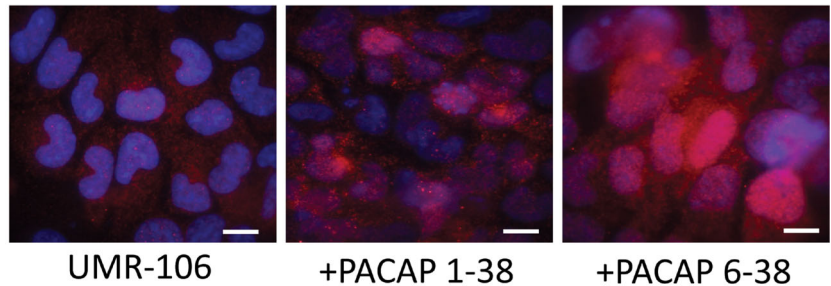
A. RT-PCR, day 4



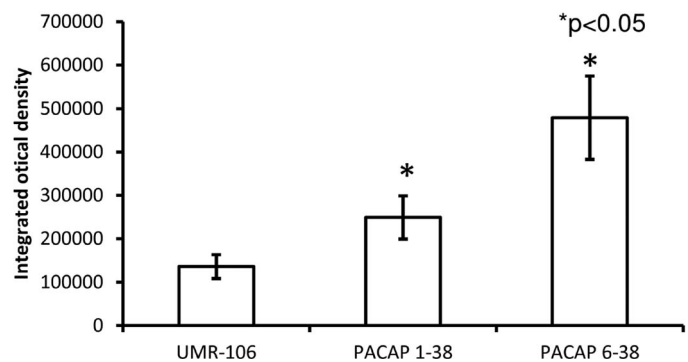
B. Western blot, day 4



C. Immunocytochemistry, day 4, Gli1



D. Densitometry of immunocytochemistry, day4, Gli1



612 data providing evidence on function of PACAP as a neuro-
 613 hormone in CNS has been reported, only sporadic data prove
 614 its origin and role in development of skeletal elements as in
 615 cartilage or bone (Juhász et al. 2014; Nagata et al. 2009;

Strange-Vognsen et al. 1997). Several results confirm the
 essential function of PACAP/VIP system in the differentiation
 or activation of osteoclasts (Nagata et al. 2009; Persson and
 Lerner 2005, 2011), and it has also been shown that PACAP/

616
 617
 618
 619

620 VIP has vital role in bone absorption (Jones et al. 2004). In our
621 experiments, low expressional level of PACAP mRNA was
622 demonstrated in UMR-106 cell line, suggesting the ability of
623 endogenous PACAP release by osteogenic cells. Under phys-
624 iological circumstances in living bone, PACAP release from
625 nerve endings in bone marrow or in periosteum is also possi-
626 ble, as it has been shown earlier (Braas et al. 2007; Strange-
627 Vognsen et al. 1997).

628 Calvaria-derived MC3T3 cells were shown to express
629 VPAC2 receptors (Nagata et al. 2009), and addition of
630 PACAP to the medium of UMR-106 cells induced cAMP
631 production (Kovacs et al. 1996). In our experiments, UMR-
632 106 cells were found to express PAC1 receptor dominantly. As
633 PAC1 has 100-fold greater affinity to bind PACAP than VIP,
634 we administrated PACAP 1-38 as an agonist and PACAP 6-38
635 as an antagonist to the medium of osteoblast cells. Without any
636 alteration on morphology or mitochondrial activity of the cells,
637 both neuropeptides increased cellular proliferation of UMR-
638 106 cells. In fact, PACAP 1-38 is known to influence prolifer-
639 ation in a tissue- and/or cell-dependent manner: it elevated the
640 proliferation of astrocytes (Nakamachi et al. 2011) and neuronal
641 progenitor cells (Nishimoto et al. 2007), but it inhibited the
642 proliferation of neuroblastoma (Waschek et al. 2000), endothe-
643 lial (Castorina et al. 2010) or Leydig cells (Matsumoto et al.
644 2008). PACAP 6-38 was reported as a potent antagonist of
645 PAC1 receptor originally (Bergstrom et al. 2003), but recent
646 data suggested its agonistic behaviour in certain conditions
647 such as in sensory nerve terminals or in cytotrophoblast cells
648 (Reglodi et al. 2008) and in glia cells (Walker et al. 2013).
649 Recently, we also reported a dominantly agonistic effect of this
650 compound in a chicken chondrogenesis model (Juhász et al.
651 2014). One can hypothesise that PACAP 6-38 may have un-
652 known effect on different isoforms of PAC1 receptor or it may
653 act on a yet unidentified PACAP receptor (Jansen-Olesen et al.
654 2014) which can activate variable signalling pathways of cells
655 (Holighaus et al. 2011).

656 As cAMP accumulation by PACAP of UMR-106 cells has
657 already been published (Kovacs et al. 1996), it could be the
658 question of interest which downstream target molecules of
659 PAC1 receptors may activate osteoblast differentiation. PKA,
660 as it is activated by the increased concentration of cAMP, is
661 one of the canonical downstream signalling targets of PACAP
662 binding (Vaudry et al. 2009), and PACAP was supposed to be
663 a positive regulator of osteogenesis via this mechanism in
664 hMSC (Siddappa et al. 2008) or in osteoblasts (Lo et al.
665 2012). CREB, a downstream target of PKA, can directly bind
666 to the promoter region of osteogenic morphogen BMP2
667 (Zhang et al. 2011). Although the expression of PKA was
668 elevated in UMR-106 cells, we were not able to detect any
669 significant alteration in the expression or in the phosphoryla-
670 tion of CREB transcription factor. Furthermore, the nuclear
671 presence of p-CREB did not show any significant change at
672 the presence of PACAPs. These results suggested an

673 alternative, CREB-independent initiation of osteogenic differ-
674 entiation. As a matter of fact, Runx2, the master transcription
675 factor of osteogenesis, can be phosphorylated by PKA and
676 ultimately can be translocated into the nucleus (Jonason et al.
677 2009; Franceschi and Xiao 2003). Although we did not find
678 any alteration of Runx2 expression after PACAP addition, its
679 nuclear localisation became pronouncedly elevated, suggest-
680 ing that it became activated by ligand binding of PAC1 recep-
681 tor and may initiate expression of osteogenic genes. Indeed,
682 we detected elevated levels of alkaline phosphatase (ALP) and
683 collagen type I mRNA and proteins following PACAP treat-
684 ments. It is also known that Runx2 can directly regulate
685 osterix expression in osteoblasts (Jonason et al. 2009). In line
686 with this observation, we found a significant elevation in
687 osterix expression under the effect of PACAPs. Both of ALP
688 and osterix can be activated by other upstream signalling
689 elements, such as Dlx5 and Smads; moreover, Runx2 can
690 cross talk with BMP signalling, and in turn, BMPs can also
691 regulate the expression of the above osteogenesis markers (Li
692 and Xiao 2007). Another proof of enhanced osteoblast differ-
693 entiation was the increased VEGF expression in our experi-
694 mental model. This growth factor is crucial for initiation of
695 vascularisation of developing bone during endochondral os-
696 sification and was capable to enhance bone formation in
697 tissue-engineered bone in animal experiments (Wu et al.
698 2013). In line with our data, it was also demonstrated that
699 VEGF expression can be regulated by the increased activity of
700 PKA (Yang et al. 2013).

701 The activation of ALP and osterix can indirectly stimulate
702 Ca^{2+} accumulation and mineralisation process in bone devel-
703 opment both in vitro and in vivo (Yan et al. 2014). There is
704 evidence in neurons that PACAP binding can activate recep-
705 tors or ion channels, generating action potential on the post-
706 synaptic cell (Aoyagi and Takahashi 2001) by changing the
707 Ca^{2+} release of cells. The vesicular transport of Ca^{2+} or the
708 Ca^{2+} release induced by PACAP has not been characterised in
709 nonexcitable cells yet, although it can be hypothesised that
710 NMDA receptors, present on osteoblast cells, may have an
711 indirect connection with PAC1 receptor activation through
712 which they can regulate Ca^{2+} inflow and/or outflow of cells
713 (MacDonald et al. 2007). Nevertheless, our results suggest
714 that PACAP binding may have an indirect effect on Ca^{2+}
715 transport of osteoblasts (Morita et al. 2002) and increase the
716 mineralisation of bone matrix. PAC1 receptor activation can
717 also result in the induction of PLC signalling pathway, which
718 subsequently may regulate IP_3 -dependent intracellular Ca^{2+}
719 release of cells as it has been demonstrated in several neuronal
720 models (Osipenko et al. 2000; Payet et al. 2003). The concen-
721 tration changes of free cytosolic Ca^{2+} ions can regulate the
722 activation of classical PKC (Hodges et al. 2006), as well as the
723 extracellular vesicular Ca^{2+} transport of cells. In UMR-106
724 cells, we were not able to detect significant alterations of
725 resting intracellular Ca^{2+} concentration by PACAPs, and the

726 Ca^{2+} -dependent PKC α was not activated, suggesting an un-
727 influenced PLC pathway of UMR-106 cells. These results
728 may further support the hypothesis that developmental
729 stage-dependent expression of different isoforms of PAC1
730 receptor results in the activation of Ca^{2+} -related or unrelated
731 downstream pathways in PACAP signalling (Yan et al. 2013).

732 One of the main regulators of bone formation is the proper
733 coexpression or sequential expression of several BMPs, in-
734 cluding BMPs 2, 4, 6 and 7 (Lavery et al. 2008). According to
735 our data, PACAP addition induced the elevation of protein
736 expression of these cytokines in UMR-106 cells. Moreover,
737 the elevated expression of BMP2 and BMP4, characterised by
738 the highest osteogenic capacity, can be responsible for the
739 induction of collagen type I expression or indirectly the in-
740 crease of mineralisation processes (Chen et al. 2012; Zouani
741 et al. 2013). Furthermore, the increase of BMP7 can be partly
742 responsible for the activation of ALP gene expression (Bei
743 et al. 2012), and indeed, we found elevated ALP mRNA and
744 protein levels after PACAP addition in our experiments.
745 BMP6 has a crucial role in regulation of osteoblast differen-
746 tiation through osterix activation (Zhu et al. 2012). Consistent
747 with this finding, BMP6 and osterix expressions both were
748 elevated following PACAP applications in our experiments.
749 The canonical pathways of BMPRI activation lead to the
750 regulation of Smad1/5/8 transcription factors and which can
751 activate expression of various bone-specific genes (Chen et al.
752 2012). We found elevated expression and nuclear presence of
753 Smad1, strongly suggesting that activation of PACAP signal-
754 ling results in the increased activity of BMP signalling in
755 UMR-106 cells, and besides activation of Runx2 by PKA,
756 this pathway also plays role in proosteogenic effect of
757 PACAPs. Moreover, activated Smad1 can cooperate with
758 Runx2 transcription factor on the promoter region of genes
759 responsible for bone formation (Drissi et al. 2003).

760 Another group of crucial osteogenesis-regulating morpho-
761 gens is the HH family consisting of three members: SHH, IHH
762 and Desert hedgehog (DHH) (Pan et al. 2013). Although the
763 functions of IHH in endochondral ossification or in cranial
764 skeleton development have been demonstrated and its presence
765 in osteoblasts has also been detected (St-Jacques et al. 1999; Tu
766 et al. 2012), we did not find any alteration in its expression after
767 PACAP administration. SHH can be responsible for proper
768 bone formation beyond its crucial role in regulation of several
769 tissue or even cancer development (Han et al. 2013; Hu et al.
770 2013; Kiuru et al. 2009). HHs can bind to Patched1 (PTCH1)
771 receptor which releases the membrane associated Smoothed
772 leading to the activation of the Gli transcription factors, which
773 ultimately translocate to the nucleus and activate target genes
774 (James et al. 2010; Pan et al. 2013). Gli1 can regulate early
775 osteogenic differentiation by the activation of Runx2 gene
776 expression (Hojo et al. 2012). SHH was also shown to have
777 an important function in neurogenic development where its
778 connection with PACAP signalling system has been published

(Waschek et al. 2000, 2006). Addition of PACAPs resulted in a
779 pronounced elevation of SHH, PTCH1, Gli1, mRNA and
780 protein levels; moreover, nuclear signal of Gli1 also became
781 stronger. Taken together, PKA and SHH pathways both were
782 found activated by PACAPs in UMR-106 cells. Nonetheless,
783 others reported antagonistic relationship of cAMP-activated
784 PKA and HH signalling during *Drosophila* development
785 (Waschek et al. 2006) and in bone formation (Regard et al.
786 2013). Moreover, PACAP was shown to inhibit the *gli1* gene
787 expression during the proliferation of medulloblastoma cells or
788 antagonise the SHH signalling pathways of motoneuron for-
789 mation in embryonic stem cell cultures (Waschek et al. 2000).
790 However, evidence about GPCR-induced SHH activation has
791 also been reported under certain circumstances and a possible
792 involvement of noncanonical SHH regulation can also
793 complicate the picture (Brennan et al. 2012). Although
794 the antagonistic communication of PKA-SHH signalling
795 pathways is convincingly proved in neuronal tissues or
796 cell types (Niewiadomski et al. 2013), the universality of this
797 way of signalling cross talk is not widely demonstrated.
798 Another possible reason which may cause the contradictory
799 expression pattern and signalling communication of PKA and
800 SHH in UMR-106 cells is the fact that this cell line originates
801 from an osteosarcoma, and HH pathways are frequently
802 overactivated in this type of tumour (Hirotzu et al. 2010).
803

804 In conclusion, this study shows that PACAP signalling
805 plays pro-osteogenic role in consecutive steps of in vitro bone
806 tissue formation via activation of various signalling pathways
807 in UMR-106 cells. This observation raises the opportunity that
808 exogenously administered PACAP may enhance bone forma-
809 tion in case of hampered fracture healings or during therapy of
810 larger bone defects in the distant future.
811

Acknowledgments The authors are grateful for Mrs. Krisztina B r 
811 and Mrs. Ella Kov acs for excellent technical assistance during the study.
812 This work was supported by grants from Akira Arimura Foundation
813 Research Grant, the Hungarian Science Research Fund (OTKA
814 CNK80709 and OTKA K 104984), Bolyai Scholarship and the
815 Hungarian Ministry of Education (T MOP 4.2.1.B-10/2/KONV-2010-
816 002, PTE-MTA "Lend ilet" Program) and from the New Sz echenyi Plan
817 (T MOP-4.2.2.A-11/1/KONV-2012-0053, T MOP-4.2.2.A-11/1/
818 KONV-2012-0024). The project is co-financed by the European Union
819 and the European Social Fund. This research and T.J. was supported by
820 the European Union and the State of Hungary, co-financed by the
821 European Social Fund in the framework of T MOP 4.2.4. A/2-11-1-
822 2012-0001 "National Excellence Program". C.M. is supported by a
823 Mecenatura grant (DEOEC Mec-9/2011) from the Medical and Health
824 Science Center, University of Debrecen, Hungary.
825

References

- 826
827
828
829
830
831
- Ago Y, Yoneyama M, Ishihama T, Kataoka S, Kawada K, Tanaka T et al
(2011) Role of endogenous pituitary adenylate cyclase-activating
polypeptide in adult hippocampal neurogenesis. *Neuroscience* 172:
554–561

- 832 Aoyagi K, Takahashi M (2001) Pituitary adenylate cyclase-activating
833 polypeptide enhances Ca(2+)-dependent neurotransmitter release
834 from PC12 cells and cultured cerebellar granule cells without affect-
835 ing intracellular Ca(2+) mobilization. *Biochem Biophys Res*
836 *Commun* 286:646–651
- 837 Bae IH, Jeong BC, Kook MS, Kim SH, Koh JT (2013) Evaluation of a
838 thiolated chitosan scaffold for local delivery of BMP-2 for osteo-
839 genic differentiation and ectopic bone formation. *Biomed Res Int*
840 2013:878930
- 841 Bastida MF, Sheth R, Ros MA (2009) A BMP-Shh negative-feedback
842 loop restricts Shh expression during limb development. *Development*
843 136:3779–3789
- 844 Bei K, Du Z, Xiong Y, Liao J, Su B, Wu L (2012) BMP7 can promote
845 osteogenic differentiation of human periosteal cells in vitro. *Mol*
846 *Biol Rep* 39:8845–8851
- 847 Bergstrom AL, Hannibal J, Hindersson P, Fahrenkrug J (2003) Light-
848 induced phase shift in the Syrian hamster (*Mesocricetus auratus*) is
849 attenuated by the PACAP receptor antagonist PACAP6-38 or
850 PACAP immunoneutralization. *Eur J Neurosci* 18:2552–2562
- 851 Borzsei R, Mark L, Tamas A, Bagoly T, Bay C, Csanaky K et al (2009)
852 Presence of pituitary adenylate cyclase activating polypeptide-38 in
853 human plasma and milk. *Eur J Endocrinol* 160:561–565
- 854 Braas KM, May V, Harakall SA, Hardwick JC, Parsons RL (1998)
855 Pituitary adenylate cyclase-activating polypeptide expression and
856 modulation of neuronal excitability in guinea pig cardiac ganglia. *J*
857 *Neurosci* 18:9766–9779
- 858 Braas KM, Schutz KC, Bond JP, Vizzard MA, Girard BM, May V (2007)
859 Microarray analyses of pituitary adenylate cyclase activating poly-
860 peptide (PACAP)-regulated gene targets in sympathetic neurons.
861 *Peptides* 28:1856–1870
- 862 Brennan D, Chen X, Cheng L, Mahoney M, Riobo NA (2012)
863 Noncanonical Hedgehog signaling. *Vitam Horm* 88:55–72
- 864 Castorina A, Giunta S, Mazzone V, Cardile V, D'Agata V (2010) Effects
865 of PACAP and VIP on hyperglycemia-induced proliferation in
866 murine microvascular endothelial cells. *Peptides* 31:2276–2283
- 867 Chen G, Deng C, Li YP (2012) TGF-beta and BMP signaling in osteo-
868 blast differentiation and bone formation. *Int J Biol Sci* 8:272–288
- 869 Drissi MH, Li X, Sheu TJ, Zuscik MJ, Schwarz EM, Puzas JE, Rosier RN
870 et al (2003) Runx2/Cbfa1 stimulation by retinoic acid is potentiated
871 by BMP2 signaling through interaction with Smad1 on the collagen
872 X promoter in chondrocytes. *J Cell Biochem* 90:1287–1298
- 873 Ehlen HW, Buelens LA, Vortkamp A (2006) Hedgehog signaling in
874 skeletal development. *Birth Defects Res C Embryo Today* 78:267–
875 279
- 876 Falluel-Morel A, Aubert N, Vaudry D, Desfeux A, Allais A, Burel D et al
877 (2008) Interactions of PACAP and ceramides in the control of
878 granule cell apoptosis during cerebellar development. *J Mol*
879 *Neurosci* 36:8–15
- 880 Forrest SM, Ng KW, Findlay DM, Michelangeli VP, Livesey SA,
881 Partridge NC et al (1985) Characterization of an osteoblast-like
882 clonal cell line which responds to both parathyroid hormone and
883 calcitonin. *Calcif Tissue Int* 37:51–56
- 884 Franceschi RT, Xiao G (2003) Regulation of the osteoblast-specific
885 transcription factor, Runx2: responsiveness to multiple signal tran-
886 sduction pathways. *J Cell Biochem* 88:446–454
- 887 Gonkowski S, Calka J (2012) Changes in pituitary adenylate cyclase-
888 activating Peptide 27-like immunoreactive nervous structures in the
889 porcine descending colon during selected pathological processes. *J*
890 *Mol Neurosci* 48(3):777–787
- 891 Gourlet P, Vandermeers A, Vertongen P, Rathe J, De NP, Cnudde J et al
892 (1997) Development of high affinity selective VIP1 receptor ago-
893 nists. *Peptides* 18:1539–1545
- 894 Han JB, Sang F, Chang JJ, Hua YQ, Shi WD, Tang LH et al (2013)
895 Arsenic trioxide inhibits viability of pancreatic cancer stem cells in
896 culture and in a xenograft model via binding to SHH-Gli. *Onco*
897 *Targets Ther* 6:1129–1138
- Hirotsu M, Setoguchi T, Sasaki H, Matsunoshita Y, Gao H, Nagao H et al 898
(2010) Smoothed as a new therapeutic target for human osteosar- 899
coma. *Mol Cancer* 12(9):5 900
- Hodges RR, Rios JD, Vrouvlianis J, Ota I, Zoukhri D, Dartt DA (2006) 901
Roles of protein kinase C, Ca2+, Pyk2, and c-Src in agonist activa- 902
tion of rat lacrimal gland p42/p44 MAPK. *Invest Ophthalmol Vis* 903
Sci 47:3352–3359 904
- Hojo H, Ohba S, Yano F, Saito T, Ikeda T, Nakajima K et al (2012) Gli1 905
protein participates in Hedgehog-mediated specification of osteo- 906
blast lineage during endochondral ossification. *J Biol Chem* 287: 907
17860–17869 908
- Holighaus Y, Mustafa T, Eiden LE (2011) PAC1hop, null and hip recep- 909
tors mediate differential signaling through cyclic AMP and calcium 910
leading to splice variant-specific gene induction in neural cells. 911
Peptides 32:1647–1655 912
- Horvath G, Mark L, Brubel R, Szakaly P, Racz B, Kiss P et al (2010) 913Q1
Mice deficient in pituitary adenylate cyclase activating polypeptide 914
display increased sensitivity to renal oxidative stress in vitro. 915
Neurosci Lett 469:70–74 916
- Horvath G, Brubel R, Kovacs K, Reglodi D, Opper B, Ferencz A et al 917
(2011) Effects of PACAP on oxidative stress-induced cell death in 918
rat kidney and human hepatocyte cells. *J Mol Neurosci* 43:67–75 919
- Hu X, Zhang S, Chen G, Lin C, Huang Z, Chen Y et al (2013) Expression 920
of SHH signaling molecules in the developing human primary 921
dentition. *BMC Dev Biol* 13:11 922
- Huang KP, Huang FL (1991) Purification and analysis of protein kinase C 923
isozymes. *Methods Enzymol* 200:241–252 924
- Inglott MA, Lerner EA, Pilowsky PM, Farnham MM (2012) Activation 925
of PAC(1) and VPAC receptor subtypes elicits differential physio- 926
logical responses from sympathetic preganglionic neurons in the 927
anaesthetized rat. *Br J Pharmacol* 167:1089–1098 928
- James AW, Leucht P, Levi B, Carre AL, Xu Y, Helms JA et al (2010) 929
Sonic Hedgehog influences the balance of osteogenesis and adipo- 930
genesis in mouse adipose-derived stromal cells. *Tissue Eng Part A* 931
16:2605–2616 932
- Jansen-Olesen I, Baun M, Amrutkar DV, Ramachandran R, 933
Christophersen DV, Olesen J (2014) PACAP-38 but not VIP induces 934
release of CGRP from trigeminal nucleus caudalis via a receptor 935
distinct from the PAC1 receptor. *Neuropeptides*. doi:10.1016/j.npep. 936
2014.01.004 937
- Jiang Q, Du J, Yin X, Shan Z, Ma Y, Ma P et al (2013) Shh signaling, 938
negatively regulated by BMP signaling, inhibits the osteo/ 939
dentinogenic differentiation potentials of mesenchymal stem cells 940
from apical papilla. *Mol Cell Biochem* 383:85–93 941
- Jolivel V, Basille M, Aubert N, de Jouffrey S, Ancian P, Le Bigot JF et al 942
(2009) Distribution and functional characterization of pituitary ade- 943
nylate cyclase-activating polypeptide receptors in the brain of non- 944
human primates. *Neuroscience* 160:434–451 945
- Jonason JH, Xiao G, Zhang M, Xing L, Chen D (2009) Post-translational 946
regulation of Runx2 in bone and cartilage. *J Dent Res* 88:693–703 947
- Jones KB, Mollano AV, Morcuende JA, Cooper RR, Saltzman CL (2004) 948
Bone and brain: a review of neural, hormonal, and musculoskeletal 949
connections. *Iowa Orthop J* 24:123–132 950
- Jozsa R, Hollosy T, Tamas A, Toth G, Lengvari I, Reglodi D (2005) 951
Pituitary adenylate cyclase activating polypeptide plays a role in 952
olfactory memory formation in chicken. *Peptides* 26:2344–2350 953
- Juhász T, Matta C, Katona E, Somogyi C, Takács R, Gergely P et al 954
(2014) Pituitary adenylate cyclase activating polypeptide (PACAP) 955
signalling exerts chondrogenesis promoting and protecting effects: 956
implication of calcineurin as a downstream target. *PLoS One* 9(3): 957
e91541 958
- Kim JH, Liu X, Wang J, Chen X, Zhang H, Kim SH et al (2013) Wnt 959
signaling in bone formation and its therapeutic potential for bone 960
diseases. *Ther Adv Musculoskelet Dis* 5:13–31 961
- Kiuru M, Solomon J, Ghali B, van der Meulen M, Crystal RG, Hidaka C 962
(2009) Transient overexpression of sonic hedgehog alters the 963

- 964 architecture and mechanical properties of trabecular bone. *J Bone*
965 *Mineral Res* 24:1598–1607
- 966 Kovacs CS, Chik CL, Li B, Karpinski E, Ho AK (1996) Pituitary
967 adenylate cyclase-activating peptide stimulates cyclic AMP accu-
968 mulation in UMR 106 osteoblast-like cells. *J Endocrinol* 149:287–
969 295
- 970 Lavery K, Swain P, Falb D, Aoui-Ismaili MH (2008) BMP-2/4 and BMP-
971 6/7 differentially utilize cell surface receptors to induce osteoblastic
972 differentiation of human bone marrow-derived mesenchymal stem
973 cells. *J Biol Chem* 283:20948–20958
- 974 Li YL, Xiao ZS (2007) Advances in Runx2 regulation and its isoforms.
975 *Med Hypotheses* 68:169–175
- 976 Lo KW, Kan HM, Ashe KM, Laurencin CT (2012) The small molecule
977 PKA-specific cyclic AMP analogue as an inducer of osteoblast-like
978 cells differentiation and mineralization. *J Tissue Eng Regen Med* 6:
979 40–48
- 980 MacDonald JF, Jackson MF, Beazely MA (2007) G protein-coupled
981 receptors control NMDARs and metaplasticity in the hippocampus.
982 *Biochim Biophys Acta* 1768:941–951
- 983 Marie PJ (2012) Fibroblast growth factor signaling controlling bone
984 formation: an update. *Gene* 498:1–4
- 985 Matsumoto S, Arakawa Y, Ohishi M, Yanaiharu H, Iwanaga T, Kurokawa
986 N (2008) Suppressive action of pituitary adenylate cyclase activat-
987 ing polypeptide (PACAP) on proliferation of immature mouse
988 Leydig cell line TM3 cells. *Biomed Res* 29:321–330
- 989 Matta C, Fodor J, Szigyarto Z, Juhasz T, Gergely P, Csemoch L et al
990 (2008) Cytosolic free Ca²⁺ concentration exhibits a characteristic
991 temporal pattern during in vitro cartilage differentiation: a possible
992 regulatory role of calcineurin in Ca-signalling of chondrogenic cells.
993 *Cell Calcium* 44:310–323
- 994 Midura RJ, McQuillan DJ, Benham KJ, Fisher LW, Hascall VC (1990) A
995 rat osteogenic cell line (UMR 106-01) synthesizes a highly sulfated
996 form of bone sialoprotein. *J Biol Chem* 265:5285–5291
- 997 Miyata A, Arimura A, Dahl RR, Minamino N, Uehara A, Jiang L et al
998 (1989) Isolation of a novel 38 residue-hypothalamic polypeptide
999 which stimulates adenylate cyclase in pituitary cells. *Biochem*
1000 *Biophys Res Commun* 164:567–574
- 1001 Morita K, Sakakibara A, Kitayama S, Kumagai K, Tanne K, Dohi T
1002 (2002) Pituitary adenylate cyclase-activating polypeptide induces a
1003 sustained increase in intracellular free Ca(2+) concentration
1004 and catechol amine release by activating Ca(2+) influx via
1005 receptor-stimulated Ca(2+) entry, independent of store-
1006 operated Ca(2+) channels, and voltage-dependent Ca(2+) channels
1007 in bovine adrenal medullary chromaffin cells. *J Pharmacol Exp Ther*
1008 302:972–982
- 1009 Nagata A, Tanaka T, Minezawa A, Poyurovsky M, Mayama T, Suzuki S
1010 et al (2009) cAMP activation by PACAP/VIP stimulates IL-6 release
1011 and inhibits osteoblastic differentiation through VPAC2 receptor in
1012 osteoblastic MC3T3 cells. *J Cell Physiol* 221:75–83
- 1013 Nakamachi T, Nakamura K, Oshida K, Kagami N, Mori H, Watanabe J
1014 et al (2011) Pituitary adenylate cyclase-activating polypeptide
1015 (PACAP) stimulates proliferation of reactive astrocytes in vitro. *J*
1016 *Mol Neurosci* 43:16–21
- 1017 Niewiadomski P, Zhujiang A, Youssef M, Waschek JA (2013)
1018 Interaction of PACAP with Sonic hedgehog reveals complex
1019 regulation of the hedgehog pathway by PKA. *Cell Signal* 25:
1020 2222–2230
- 1021 Nishimoto M, Furuta A, Aoki S, Kudo Y, Miyakawa H, Wada K (2007)
1022 PACAP/PAC1 autocrine system promotes proliferation and
1023 astrogenesis in neural progenitor cells. *Glia* 55:317–327
- 1024 Ochiai T, Shibukawa Y, Nagayama M, Mundy C, Yasuda T, Okabe T et al
1025 (2010) Indian hedgehog roles in post-natal TMJ development and
1026 organization. *J Dent Res* 89:349–354
- 1027 Ohta S, Gregg C, Weiss S (2006) Pituitary adenylate cyclase-activating
1028 polypeptide regulates forebrain neural stem cells and neurogenesis
1029 in vitro and in vivo. *J Neurosci Res* 84:1177–1186
- Ok CY, Singh RR, Vega F (2012) Aberrant activation of the hedgehog
1030 signaling pathway in malignant hematological neoplasms. *Am J*
1031 *Pathol* 180:2–11
- Osipenko ON, Barrie AP, Allen JM, Gurney AM (2000) Pituitary
1032 adenylate cyclase-activating peptide activates multiple intracellular
1033 signaling pathways to regulate ion channels in PC12 cells. *J Biol*
1034 *Chem* 275:16626–16631
- 1035 Pan A, Chang L, Nguyen A, James AW (2013) A review of hedgehog
1036 signaling in cranial bone development. *Front Physiol* 4:61
- 1037 Payet MD, Bilodeau L, Breault L, Fournier A, Yon L, Vaudry H et al
1038 (2003) PAC1 receptor activation by PACAP-38 mediates Ca²⁺
1039 release from a cAMP-dependent pool in human fetal adrenal gland
1040 chromaffin cells. *J Biol Chem* 278:1663–1670
- 1041 Perrier-Groult E, Padeloup M, Malbouyres M, Galera P, Mallein-Gerin F
1042 (2013) Control of collagen production in mouse chondrocytes by
1043 using a combination of bone morphogenetic protein-2 and small
1044 interfering RNA targeting Col1a1 for hydrogel-based tissue-
1045 engineered cartilage. *Tissue Eng Part C Methods* 19:652–664
- 1046 Persson E, Lerner UH (2005) The neuropeptide VIP potentiates IL-6
1047 production induced by proinflammatory osteotropic cytokines in
1048 calvarial osteoblasts and the osteoblastic cell line MC3T3-E1.
1049 *Biochem Biophys Res Commun* 335:705–711
- 1050 Persson E, Lerner UH (2011) The neuropeptide VIP regulates the expres-
1051 sion of osteoclastogenic factors in osteoblasts. *J Cell Biochem* 112:
1052 3732–3741
- 1053 Pirone A, Baoan D, Piano I, Santana LD, Baglini A, Lenzi C (2011)
1054 Pituitary adenylate cyclase-activating peptide (PACAP) immunore-
1055 activity distribution in the small intestine of the adult New
1056 Hampshire chicken. *Acta Histochem* 113:477–483
- 1057 Regard JB, Malhotra D, Gvozdenovic-Jeremic J, Josey M, Chen M,
1058 Weinstein LS et al (2013) Activation of Hedgehog signaling by loss
1059 of GNAS causes heterotopic ossification. *Nat Med* 19:1505–1512
- 1060 Reglodi D, Borzsei R, Bagoly T, Boronkai A, Racz B, Tamas A et al
1061 (2008) Agonistic behavior of PACAP6-38 on sensory nerve termi-
1062 nals and cytotrophoblast cells. *J Mol Neurosci* 36:270–278
- 1063 Reglodi D, Gyarmati J, Ertl T, Borzsei R, Bodis J, Tamas A et al (2010)
1064 Alterations of pituitary adenylate cyclase-activating polypeptide-
1065 like immunoreactivity in the human plasma during pregnancy and
1066 after birth. *J Endocrinol Investig* 33:443–445
- 1067 Reglodi D, Kiss P, Horvath G, Lubics A, Laszlo E, Tamas A et al (2011)
1068 Effects of pituitary adenylate cyclase activating polypeptide in the
1069 urinary system, with special emphasis on its protective effects in the
1070 kidney. *Neuropeptides* 46:61–70
- 1071 Reglodi D, Tamas A, Koppan M, Szogyi D, Welke L (2012) Role of
1072 PACAP in female fertility and reproduction at gonadal level—recent
1073 advances. *Front Endocrinol (Lausanne)* 11(3):155
- 1074 Sanchez A, Chiriva-Internati M, Grammas P (2008) Transduction of
1075 PACAP38 protects primary cortical neurons from neurotoxic injury.
1076 *Neurosci Lett* 448:52–55
- 1077 Seeliger S, Buddenkotte J, Schmidt-Choudhury A, Rosignoli C,
1078 Shpacovitch V, von Arnim U et al (2010) Pituitary adenylate cyclase
1079 activating polypeptide: an important vascular regulator in human
1080 skin in vivo. *Am J Pathol* 177:2563–2575
- 1081 Shioda S, Legradi G, Leung WC, Nakajo S, Nakaya K, Arimura A (1994)
1082 Localization of pituitary adenylate cyclase-activating polypeptide
1083 and its messenger ribonucleic acid in the rat testis by light and
1084 electron microscopic immunocytochemistry and in situ hybridiza-
1085 tion. *Endocrinology* 135:818–825
- 1086 Shioda S, Ohtaki H, Nakamachi T, Dohi K, Watanabe J, Nakajo S et al
1087 (2006) Pleiotropic functions of PACAP in the CNS: neuroprotection
1088 and neurodevelopment. *Ann N Y Acad Sci* 1070:550–560
- 1089 Shpakov AO, Derkach KV, Chistiakova OV, Bondareva VM (2011)
1090 Functional state of adenylate cyclase signaling system in testis and
1091 ovary of fasted rats. *Zh Evol Biokhim Fiziol* 47:40–48
- 1092 Siddappa R, Martens A, Doorn J, Leusink A, Olivo C, Licht R et al
1093 (2008) cAMP/PKA pathway activation in human mesenchymal
1094 1095

- 1096 stem cells in vitro results in robust bone formation in vivo. *Proc Natl*
1097 *Acad Sci U S A* 105:7281–7286
- 1098 St-Jacques B, Hammerschmidt M, McMahon AP (1999) Indian hedge-
1099 hog signaling regulates proliferation and differentiation of
1100 chondrocytes and is essential for bone formation. *Genes Dev* 13:
1101 2072–2086
- 1102 Strange-Vognsen HH, Ambjerg J, Hannibal J (1997) Immunocytochemical
1103 demonstration of pituitary adenylate cyclase activating polypeptide
1104 (PACAP) in the porcine epiphyseal cartilage canals. *Neuropeptides*
1105 31:137–141
- 1106 Tamas A, Reglodi D, Farkas O, Kovessi E, Pal J, Povolishock JT et al
1107 (2012) Effect of PACAP in Central and Peripheral Nerve Injuries.
1108 *Int J Mol Sci* 13:8430–8448
- 1109 Toriyama M, Mizuno N, Fukami T, Iguchi T, Toriyama M, Tago K et al
1110 (2012) Phosphorylation of doublecortin by protein kinase A orches-
1111 trates microtubule and actin dynamics to promote neuronal progen-
1112 itor cell migration. *J Biol Chem* 287:12691–12702
- 1113 Tu X, Joeng KS, Long F (2012) Indian hedgehog requires additional
1114 effectors besides Runx2 to induce osteoblast differentiation. *Dev*
1115 *Biol* 362:76–82
- 1116 Vandermeers A, Vandenborre S, Hou X, De NP, Robberecht P,
1117 Vandermeers-Piret MC et al (1992) Antagonistic properties are
1118 shifted back to agonistic properties by further N-terminal shortening
1119 of pituitary adenylate-cyclase-activating peptides in human neuro-
1120 blastoma NB-OK-1 cell membranes. *Eur J Biochem* 208:815–819
- 1121 Vaudry D, Falluel-Morel A, Bourgault S, Basille M, Burel D, Wurtz O
1122 et al (2009) Pituitary adenylate cyclase-activating polypeptide and
1123 its receptors: 20 years after the discovery. *Pharmacol Rev* 61:283–
1124 357
- 1125 Vazin T, Ashton RS, Conway A, Rode NA, Lee SM, Bravo V et al (2014)
1126 The effect of multivalent Sonic hedgehog on differentiation of
1127 human embryonic stem cells into dopaminergic and GABAergic
1128 neurons. *Biomaterials* 35(3):941–948
- 1129 Wada Y, Nakamachi T, Endo K, Seki T, Ohtaki H, Tsuchikawa D et al
1130 (2013) PACAP attenuates NMDA-induced retinal damage in asso-
1131 ciation with modulation of the microglia/macrophage status into an
1132 acquired deactivation subtype. *J Mol Neurosci* 51(2):493–502
- 1133 Walker CS, Sundrum T, Hay DL (2013) PACAP receptor pharmacology
1134 and agonist bias: Analysis in primary neurons and glia from the
1135 trigeminal ganglia and transfected cells. *Br J Pharmacol* 171:1521–
1136 1533
- 1178
- Wang L, Park P, La MF, Than K, Rahman S, Lin CY (2013) Bone
1137 formation induced by BMP-2 in human osteosarcoma cells. *Int J*
1138 *Oncol* 43:1095–1102
- Waschek JA, Cicco-Bloom EM, Lelievre V, Zhou X, Hu Z (2000)
1140 PACAP action in nervous system development, regeneration, and
1141 neuroblastoma cell proliferation. *Ann NY Acad Sci* 921:129–136
- 1142 Waschek JA, Cicco-Bloom E, Nicot A, Lelievre V (2006) Hedgehog
1143 signaling: new targets for GPCRs coupled to cAMP and protein
1144 kinase A. *Ann NY Acad Sci* 1070:120–128
- 1145 Watanabe J, Nakamachi T, Matsuno R, Hayashi D, Nakamura M,
1146 Kikuyama S et al (2007) Localization, characterization and function
1147 of pituitary adenylate cyclase-activating polypeptide during brain
1148 development. *Peptides* 28:1713–1719
- 1149 Wu X, Hou T, Luo F, Xing J, He Q, Jin H et al (2013) Vascular endothelial
1150 growth factor and physiological compressive loading synergistically
1151 promote bone formation of tissue-engineered bone. *Tissue Eng Part*
1152 *A* 19:2486–2494
- 1153 Yan Y, Zhou X, Pan Z, Ma J, Waschek JA, DiCicco-Bloom E (2013) Pro-
1154 and anti-mitogenic actions of pituitary adenylate cyclase-activating
1155 polypeptide in developing cerebral cortex: potential mediation by
1156 developmental switch of PAC1 receptor mRNA isoforms. *J*
1157 *Neurosci* 33(9):3865–3878
- 1158 Yan XZ, Yang W, Yang F, Kersten-Niessen M, Jansen JA, Both SK
1159 (2014) Effects of continuous passaging on mineralization of
1160 MC3T3-E1 cells with improved osteogenic culture protocol tissue.
1161 *Eng Part C Methods* 20(3):198–204
- 1162 Yang J, Shi QD, Song TB, Feng GF, Zang WJ, Zong CH et al (2013)
1163 Vasoactive intestinal peptide increases VEGF expression to
1164 promote proliferation of brain vascular endothelial cells via
1165 the cAMP/PKA pathway after ischemic insult in vitro. *Peptides* 42:
1166 105–111
- 1167 Zhang R, Edwards JR, Ko SY, Dong S, Liu H, Oyajobi BO et al
1168 (2011) Transcriptional regulation of BMP2 expression by the
1169 PTH-CREB signaling pathway in osteoblasts. *PLoS One* 6:
1170 e20780
- 1171 Zhu F, Friedman MS, Luo W, Woolf P, Hankenson KD (2012)
1172 The transcription factor osterix (SP7) regulates BMP6-induced
1173 human osteoblast differentiation. *J Cell Physiol* 227:2677–2685
- 1174 Zouani OF, Rami L, Lei Y, Durrieu MC (2013) Insights into the osteoblast
1175 precursor differentiation towards mature osteoblasts induced by
1176 continuous BMP-2 signaling. *Biol Open* 2:872–881
- 1177

AUTHOR QUERIES

AUTHOR PLEASE ANSWER ALL QUERIES.

- Q1. Horvath et al. (2010) was not cited anywhere in the text. Please provide a citation. Alternatively, delete the item from the list.
- Q2. Ok et al. (2012) was not cited anywhere in the text. Please provide a citation. Alternatively, delete the item from the list.
- Q3. Reglodi et al. (2011) was not cited anywhere in the text. Please provide a citation. Alternatively, delete the item from the list.

UNCORRECTED PROOF